THE ASTROPHYSICAL JOURNAL, 311:275–298, 1986 December 1

IDENTIFICATION OF TWO SOUTHERN X-RAY EMITTING CATACLYSMIC VARIABLES

I. R. TUOHY AND D. A. H. BUCKLEY
Mount Stromlo and Siding Spring Observatories, Australian National University
R. A. REMILLARD AND H. V. BRADT
Massachusetts Institute of Technology
AND
D. A. SCHWARTZ
Harvard-Smithsonian Center for Astrophysics
Received 1985 December 9; accepted 1986 May 14

ABSTRACT

We report the optical identification of two faint *HEAO 1* X-ray sources with previously uncataloged cataclysmic variables. The identifications were made on the basis of positional data provided by the *HEAO 1* Scanning Modulation Collimator experiment. The two cataclysmic variables, 1H 0542−407 and H0534−581, have average V magnitudes of ∼15.7 and ∼14.9, and have similar high excitation spectra with moderate to strong He II λ4686 emission.

We have undertaken *EXOSAT* X-ray measurements and multicolor optical photometry for both objects. These observations establish 1H 0542−407 as a new DQ Herculis magnetic variable having a white dwarf rotation period of ∼1920 s and an orbital period near 6.2 hr. 1H 0542−407 is unusual among DQ Her systems in having a large soft X-ray pulse fraction of ∼70% semiamplitude below 1 keV. No definitive X-ray or optical periodicities were detected from H0534−581, but it appears to be either a nova-like variable or a DQ Her system. Last, we note that both cataclysmic variables have very hard X-ray spectra ($kT \geq 10$ keV), with evidence for iron line emission at ∼6.7 keV from 1H 0542−407.

Subject headings: stars: dwarf novae — stars: magnetic — stars: X-rays — X-rays: binaries

I. INTRODUCTION

Although the active mission of the *HEAO 1* satellite terminated in 1979, ongoing analysis of data from the Scanning Modulation Collimator (MC) experiment (Gursky *et al.* 1978; Schwartz *et al.* 1978) continues to yield important new positional results. Aided by coarse X-ray positions (few tenths of a square degree) that have recently become available from the *HEAO 1* Large Area Sky Survey A-1 experiment (Wood *et al.* 1984), we have produced error diamonds for about 300 sources having 2–10 keV fluxes as weak as 2×10^{-11} ergs cm^{-2} s^{-1}, or roughly 1 μJy at 4 keV. The multiple, diamond-shaped MC locations reduce the positional uncertainty by a factor 10–80, depending on the significance of detection. Schwartz *et al.* (1985) discuss how the independent source existence measurement of the A-1 experiment allows the MC to produce reliable positions down to a 3 σ threshold.

We are attempting to identify as many optical counterparts of the fainter A-3 sources as possible to determine relative source populations and to isolate objects of particular astrophysical interest. The search techniques being used are described in detail by Remillard *et al.* (1986). Most of our identifications have been of BL Lac objects and other active galactic nuclei (Schwartz *et al.* 1984*a*; Remillard *et al.* 1986), with significant numbers of sources also identified with stellar objects such as RS CVn systems (Buckley *et al.* 1986) and Be star binaries. We have recently discovered four new cataclysmic variables (preliminary announcements by Schwartz *et al.* 1984*b* and Tuohy *et al.* 1985), in addition to six earlier MC discoveries. This paper discusses the identification, and subsequent X-ray (*EXOSAT*) and optical observations, of the two new southern objects, 1H 0542−407 and H0534−581.

II. OPTICAL IDENTIFICATION AND SPECTROSCOPY

a) 1H 0542−407

1H 0542−407 was discovered by the *HEAO* A-1 experiment (Wood *et al.* 1984) and was also detected by the A-3 experiment at significance levels of 2.4 σ and 4.0 σ in the 30″ (MC1) and 2′ (MC2) modulation collimator arrays respectively. The A-3 results were obtained by summing the 0.9–5.5 keV data from three 11 day scans of the source during the period 1977–1979. We estimate the 2–10 keV flux as 2.1×10^{-11} ergs cm^{-2} s^{-1}, based on the countrate in the A-1 detectors (Wood *et al.* 1984). Figure 1*a* depicts the A-1 and A-3 error regions for the source. As part of our procedure to isolate UV-excess objects, we obtained a double exposure U/B plate of the field using the 26″/20″ Uppsala Schmidt telescope at Siding Spring Observatory. Inspection of the plate revealed a very blue star lying near the center of an A-3 error diamond, although well outside the A-1 error box.[1] A finding chart and coordinates for the object are given in Figure 2*a*.

A low-resolution (∼10 Å FWHM) spectrum of the candidate star was obtained on 1984 October 19 using the 3.9 m Anglo-Australian Telescope (AAT) and the RGO spectrograph with the Image Photon Counting System (IPCS). The seeing was ≲1″.5, and the spectrograph slit of projected width 2″ was aligned at a position angle of 196° to exclude light from a

[1] We have reviewed the positions of previously identified, faint *HEAO 1* sources for comparison with their respective A-1 error boxes, and we conclude that the A-1 boxes are significantly underestimated. The RMS deviations in the positions of *HEAO* A-3 identifications, and also identifications claimed in the A-1 catalog itself (Wood *et al.* 1984), require an increase in area by a factor ∼3.5 if the A-1 error boxes are to contain 90% of the optical counterparts.

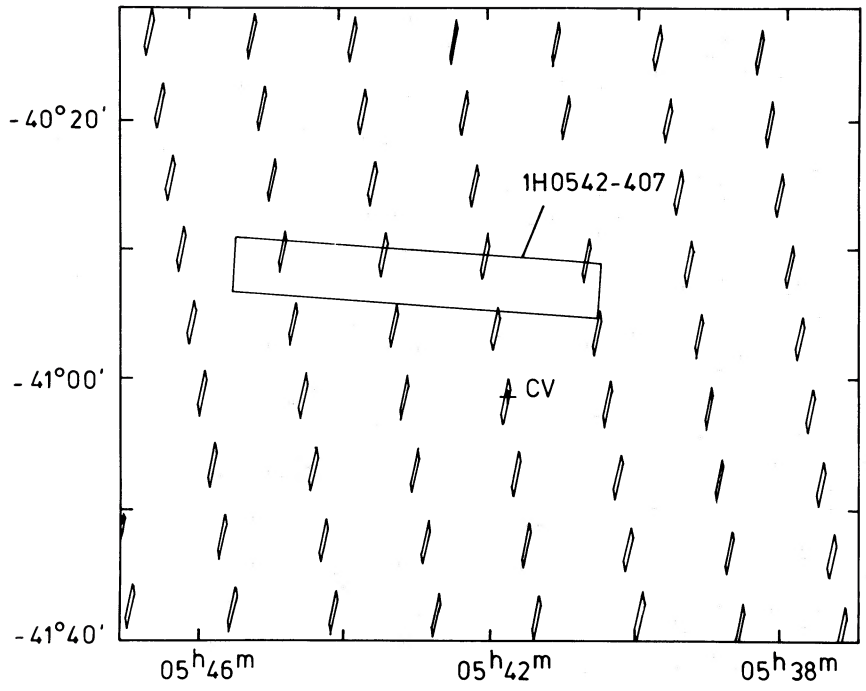

FIG. 1a

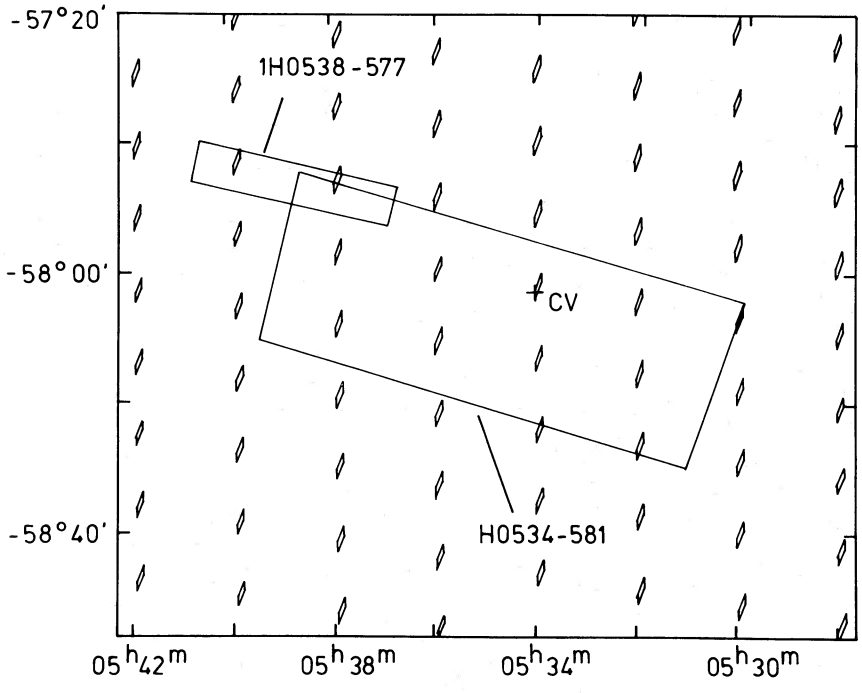

FIG. 1b

FIG. 1.—(*a*) *HEAO* A-1 error box and the multiple A-3 diamonds for 1H 0542−407. A cross indicates the location of the cataclysmic variable. (*b*) X-ray error boxes for H0534−581 determined by the *HEAO* A-2 (H0534−581) and *HEAO* A-1 (1H 0538−577) experiments, shown with the A-3 error diamonds. The position of the cataclysmic variable is marked by a cross.

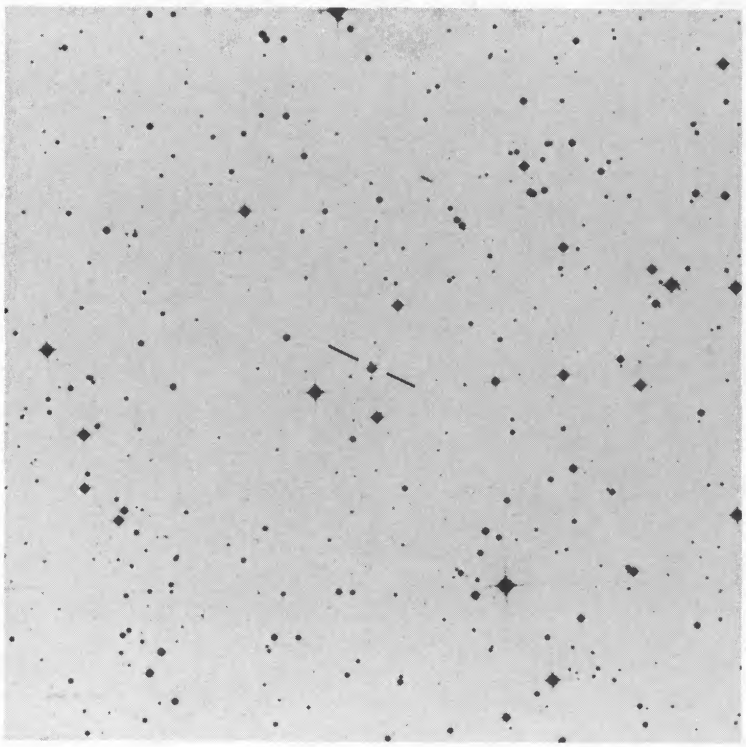

FIG. 2a

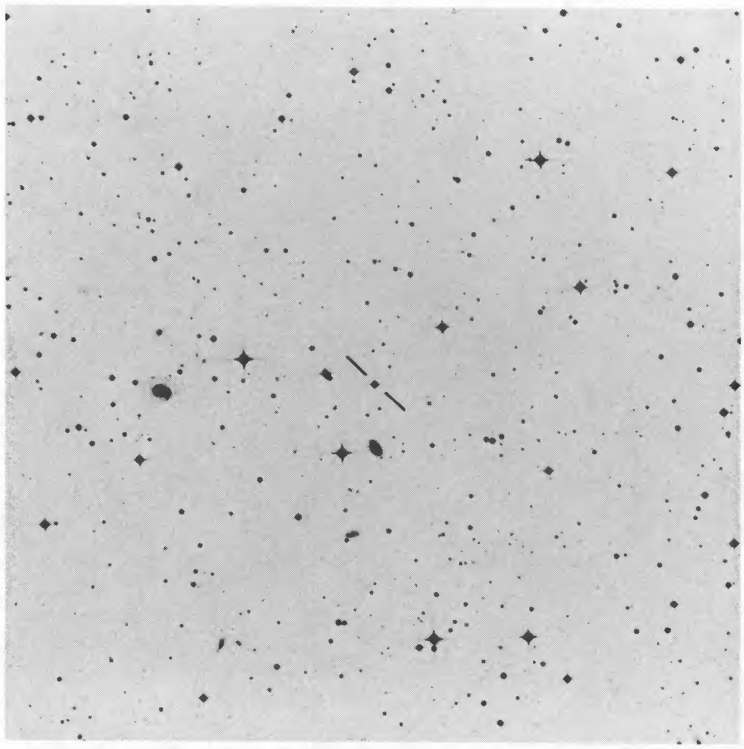

FIG. 2b

FIG. 2.—Finding charts for 1H 0542−407 (*a*) and H0534−581 (*b*) reproduced from the SRC-J survey. The dimensions of each chart are approximately 14′ × 14′. North is at the top, and east is to the left. The 1950 positions of the two cataclysmic variables, measured by the AAT, are 1H 0542−407: $\alpha = 05^{h}41^{m}44^{s}.5$, $\delta = -41°03'13''$; and H0534−581: $\alpha = 05^{h}34^{m}02^{s}.4$, $\delta = -58°03'33''$. Note that for 1H 0542−407, the optical counterpart is the easternmost of the unresolved pair (separation ∼3″).

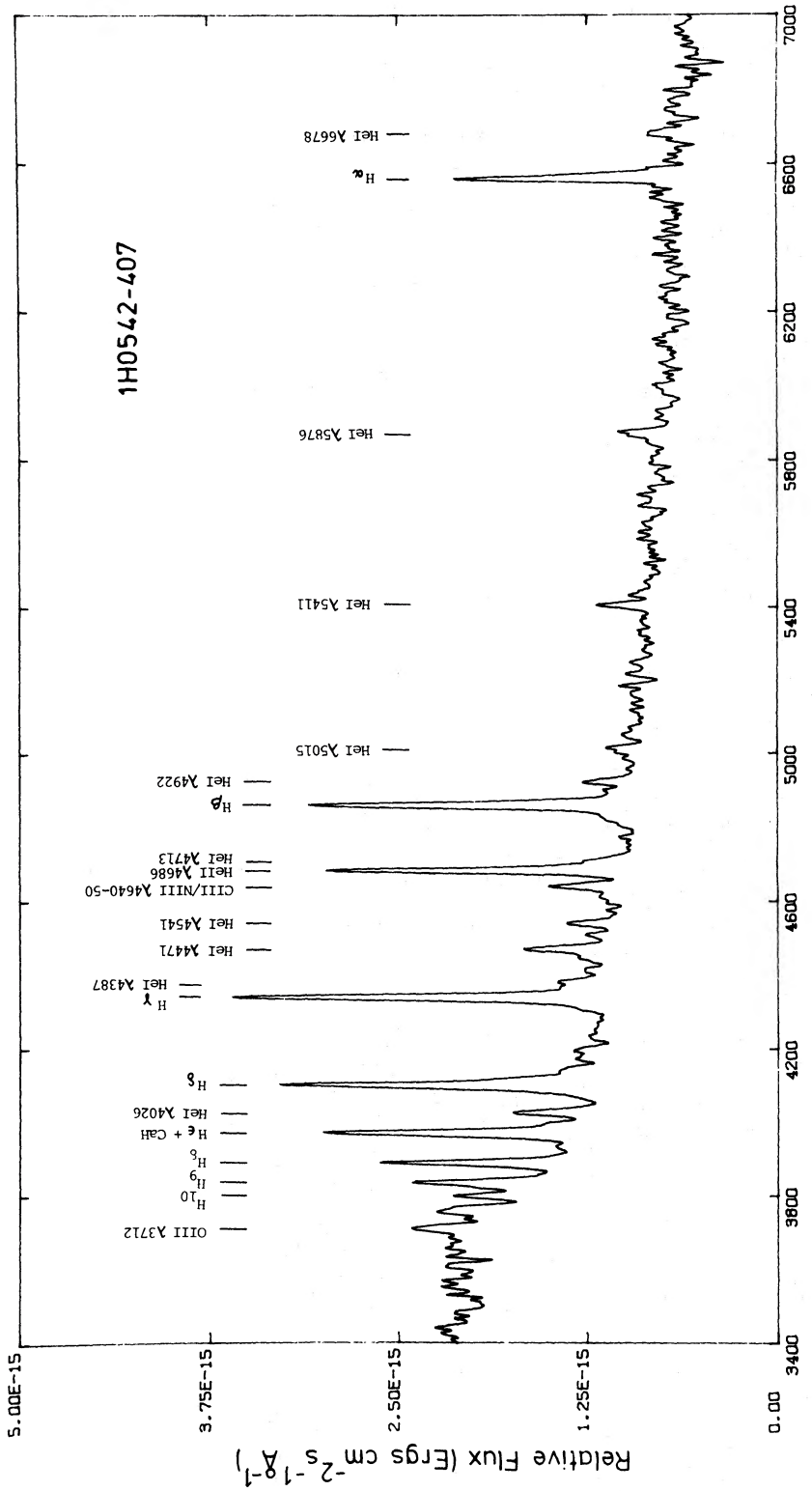

FIG. 3*a*.—AAT spectrum of 1H 0542−407 obtained on 1984 October 19, 1724–1734 UT

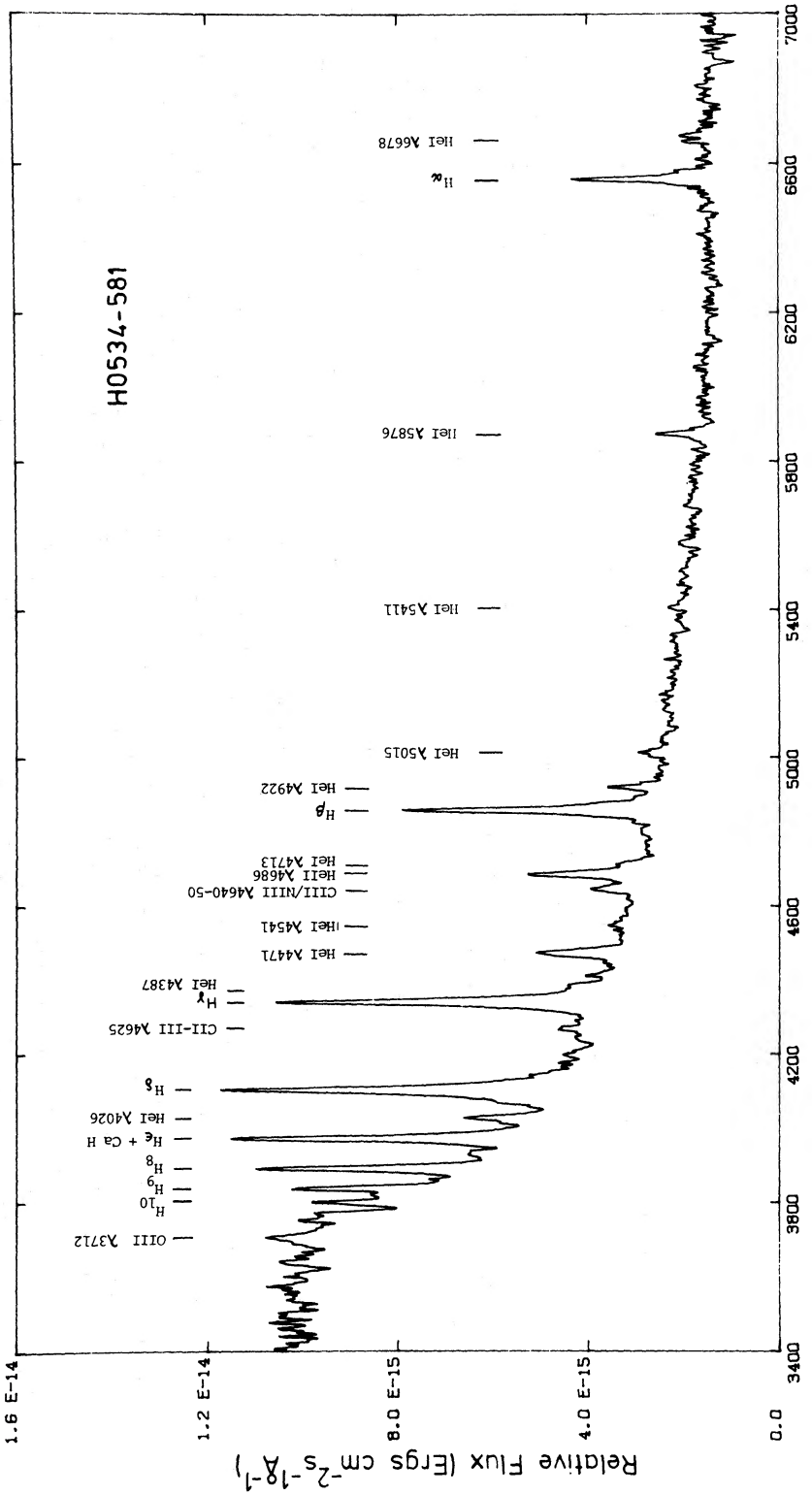

FIG. 3*b*.—AAT spectrum of H0534 − 581 obtained on 1984 February 8, 1207–1232 UT

TABLE 1

EMISSION-LINE PARAMETERS

Identification		1H 0542−407			H0534−581		
Line	λ	Intensity with Respect to Hβ	EW (Å)	FWHM (km s^{-1})	Intensity with Respect to Hβ	EW (Å)	FWHM (km s^{-1})
H10	λ3798	13.1 ± 2.84	3.6 ± 0.8	1101 ± 111	19.0 ± 3.3	2.7 ± 0.4	942 ± 92
H9	λ3835	33.0 ± 3.5	9.8 ± 1.0	1090 ± 110	38.20 ± 4.0	5.9 ± 0.6	933 ± 91
H8	λ3889	49.7 ± 2.5	16.6 ± 0.8	1063 ± 49	74.0 ± 3.6	13.1 ± 0.5	1134 ± 42
Hϵ	λ3970	80.5 ± 2.5	27.7 ± 0.8	1297 ± 32	107.9 ± 4.6	21.6 ± 0.6	1242 ± 34
He I	λ4026	17.9 ± 21.	6.5 ± 0.8	1018 ± 117	18.4 ± 2.3	4.0 ± 0.5	962 ± 119
Hδ–C III	λ4101	110.0 ± 4.0	41.5 ± 1.5	1419 ± 48	165.9 ± 7.8	39.2 ± 1.5	1722 ± 60
Hγ	λ4340	112.2 ± 2.9	44.2 ± 1.0	1104 ± 24	140.6 ± 5.5	40.4 ± 1.0	1373 ± 34
He I	λ4471	20.4 ± 2.0	8.1 ± 0.8	964 ± 95	39.5 ± 2.0	13.6 ± 0.6	1332 ± 47
C III–N III	λ4645	13.4 ± 1.9	5.8 ± 0.8	...	18.1 ± 1.6	7.0 ± 0.6	1282 ± 44
He II	λ4686	82.4 ± 2.7	37.1 ± 1.1	924 ± 29	50.6 ± 2.3	20.1 ± 0.7	1270 ± 44
Hβ	λ4861	100.0	46.0 ± 0.9	1016 ± 18	100.0	41.5 ± 1.4	1141 ± 36
He I	λ4922	9.8 ± 1.9	4.5 ± 0.9	784 ± 154	10.9 ± 1.2	4.7 ± 0.5	636 ± 74
He I	λ5876	...	...	...	16.1 ± 1.7	12.1 ± 1.3	694 ± 75
Hα	λ6563	66.8 ± 4.4	45.7 ± 3.3	729 ± 51	47.8 ± 2.9	36.2 ± 2.1	740 ± 43

NOTE.—FWZI $\approx$ 3000 km s^{-1} at Hβ for both H0534−581 and 1H 0542−407.

nearby star of comparable brightness lying $\sim$3″ to the west. Figure 3*a* shows the spectrum which has been calibrated using a white dwarf standard (L745−46A; Oke 1974). The object is unquestionably a cataclysmic variable and is distinguished by having particularly intense He II λ4686 emission. All of the emission lines show broad and narrow components, with the broad components contributing $\sim$20% to the total line fluxes. We have fitted the individual emission lines with double Gaussian profiles to produce the equivalent widths and velocity widths summarized in Table 1.

Immediately after our observation of 1H 0542−407, we obtained a brief spectrum of the neighboring star lying to the west. The spectrum is free of contaminating emission lines from the cataclysmic variable and shows the star to be late-type, with an approximate spectral classification of F/G. Integration of our spectra for both 1H 0542−407 and the neighboring star shows that the relative V magnitudes of both objects were identical to within 0.1 mag at the time of the two measurements. This information is used later in the paper for determining approximate photometric magnitudes of the two stars.

Additional AAT observations of 1H 0542−407 were undertaken on 1984 December 15 using the Pockels Cell Spectropolarimeter to search for polarization. This instrument and the associated data analysis procedure are described by McClean *et al.* (1984). Our medium-resolution ($\sim$5 Å FWHM) spectrum and the accompanying circular polarization data are displayed in Figure 4. No polarization was detected, and we can set a 3 σ upper limit of 1% to the mean circular polarization between 4000 and 6000 Å.

b) H0534−581

H0534−581 was discovered by Marshall *et al.* (1979) in the *HEAO* A-2 data base. It was also detected by the A-1 experiment (1H 0534−577; Wood *et al.* 1984), and by the A-3 modulation collimator arrays at significance levels of 3.5 σ (MC1) and 5.2 σ (MC2). The A-3 detections were obtained by summing the 2.5–13 keV data from three 30 day scans over the source region. We estimate the equivalent 2–10 keV flux at 2.8×10^{-11} ergs cm^{-2} s^{-1}. The A-1 and A-2 error boxes and multiple A-3 error diamonds are shown in Figure 1*b*. A very blue $\sim$15 mag star was isolated from a U/B plate of the field taken using the 36″/24″ Schmidt telescope at CTIO. The candidate lies at the edge of an A-3 error diamond, which itself lies near the center of the A-2 box, but outside both dimensions of the A-1 box. The coordinates and finding chart for the object are given in Figure 2*b*.

A low-resolution spectrum of the candidate star was obtained on 1984 February 4 using the 60″ telescope at CTIO. This spectrum clearly showed the object to be a cataclysmic variable. Subsequently, on 1984 February 8, we obtained three consecutive 500 s spectra of the star using the AAT. The combined AAT spectrum has been calibrated using an Oke standard (L745−46A) and is depicted in Figure 3*b*. Moderately strong He II λ4686 emission is evident, together with the usual intense emission lines and blue continuum typical of many cataclysmic variables. All of the emission lines show a broad and a narrow component, with the broad component accounting for $\sim$20% of the total flux in the line. Parameters for the emission lines, determined using the same procedure as for 1H 0542−407, are included in Table 1.

III. *EXOSAT* OBSERVATIONS

Following our identification of 1H 0542−407 and H0534−581 as cataclysmic variables, both objects were observed by *EXOSAT* to investigate their X-ray temporal and spectral properties. *EXOSAT* is ideal for such studies of cataclysmic variables, since the 3^{d}.8 spacecraft orbit allows long exposures which are uninterrupted by Earth occultation. Accordingly, 1H 0542−407 and H0534−581 were observed continuously for $\sim$12 hr and $\sim$8 hr, respectively. Simultaneous optical photometry from Siding Spring Observatory was attempted for both sources, but was only successful for H0534−581.

The *EXOSAT* data from the LE1/CMA telescope (de Korte *et al.* 1981) and the ME experiment (Turner, Smith, and Zimmerman 1981) were analyzed using the Interactive Analysis System at the European Space Operations Center (ESOC). Additional reduction of time series files produced by the ESOC software was undertaken at MSSSO. It is remarked at the outset that since these files contain time discontinuities, the

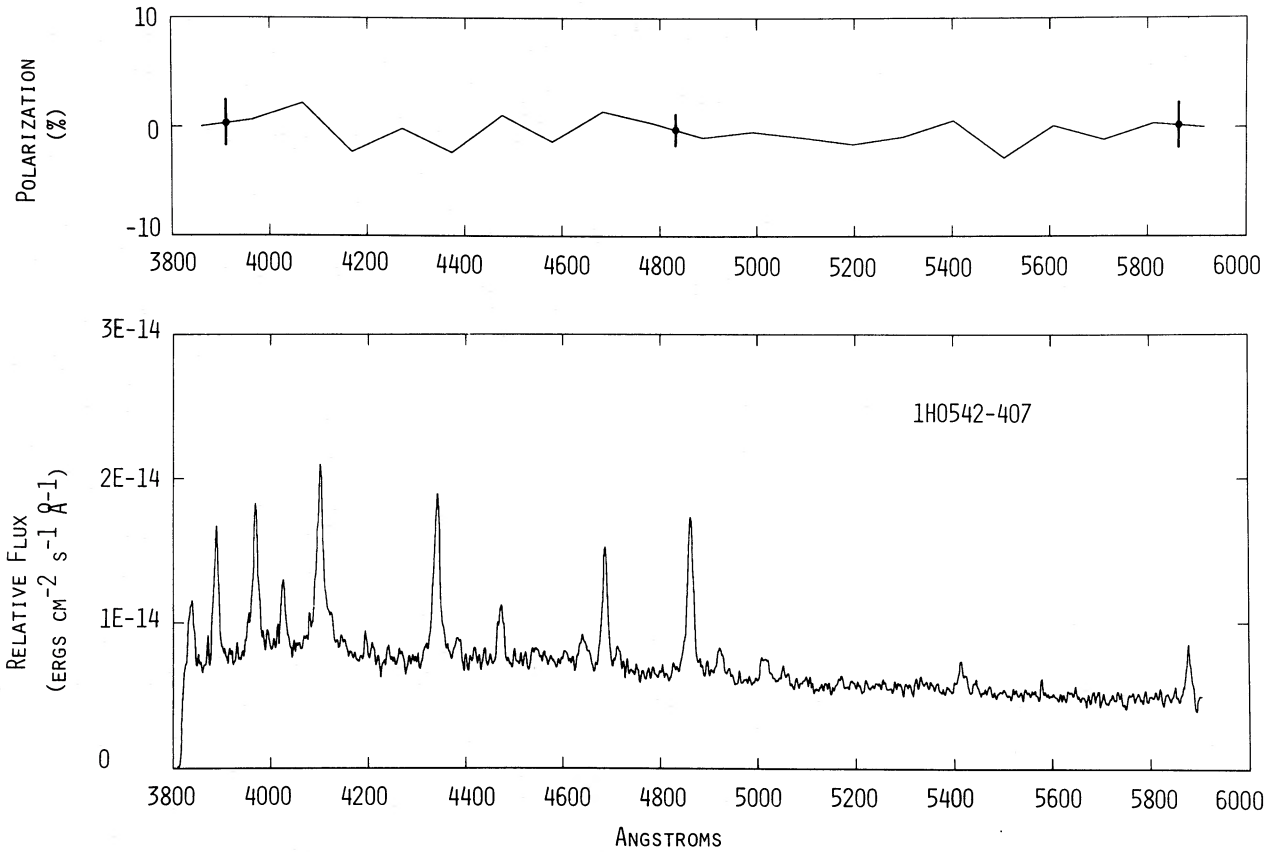

FIG. 4.—Spectropolarimetry of 1H 0542−407 obtained using the AAT on 1984 December 15, 1624–1659 UT. The circular polarization data in the upper panel have been binned into ~100 Å intervals, and representative ±1 σ error bars are plotted.

temporal analysis was accomplished by epoch folding rather than by using Fourier techniques (the same situation applies for the optical data reported later in § IV).

a) 1H 0542−407 X-Ray Image

An X-ray image of the 1H 0542−407 field was obtained with LE1 on 1985 February 23, 0307–1501 UT, using the 3000 Lexan filter, which provides broad-band sensitivity between 0.1 and 1 keV. This exposure revealed a prominent point X-ray source of intensity 0.0102 ± 0.0006 counts s^{-1} lying at a position of $\alpha = 05^h41^m45^s.1$, $\delta = -41°03'04''.0$ (1950.0). The cataclysmic variable (§ II*a*) lies within the ~15″ error radius for the X-ray position. Thus our identification of the *HEAO 1* X-ray source is confirmed. We note that a second X-ray source having an LE1 intensity of 0.0039 ± 0.0007 counts s^{-1} was detected 13.′6 to the north of the cataclysmic variable. Since this source, designated as EXO 054147−4049.5, is a factor of ~2.6 fainter than the cataclysmic variable, it is not likely to have significantly affected the *HEAO 1* detections.[2]

b) 1H 0542−407 Time Series Analysis

Time series data from the LE1 exposure of 1H 0542−407 were produced by subtracting the background contribution (averaged over an annular region centered on the source) from a circular area containing the source and binning the residual counts into 10 s samples. A plot of the resulting data (Fig. 5*a*) showed immediately the presence of strong and persistent pulsations of variable amplitude at a period near 2000 s. Accordingly, the data were folded over a range of trial periods between 100 and 10,000 s to investigate the modulation. The folded light curves were tested against a constant source model, and the ensuing plot of chi-squared (χ^2) versus period for the range 1500–2500 s is shown in Figure 6*a*. A dominant χ^2 peak is evident at a period of 1920 ± 20 s, together with a second well-resolved peak at 2084 ± 30 s. No other peaks of comparable amplitude were found at other periods. The folded light curve corresponding to the 1920 s periodicity is displayed in Figure 7*a*. The light curve is closely sinusoidal, with a pulse fraction of ~70% semiamplitude.

The object 1H 0542−407 was also viewed contemporaneously by the *EXOSAT* ME detectors between 0235 and 1522 UT. The two offset array halves (H1 and H2) measuring the source and a nearby background region were interchanged during the observation such that both H1 and H2 recorded two asynchronous pairs of source—background cycles. This procedure minimizes systematic errors in the background determination, and except for brief detector movements, the source was always being monitored by either H1 or H2. Thus, by allowing for slight differences in the relative responses of the two arrays, it was possible to construct a continuous time series file of source intensity in 10 s samples, and also a combined measurement of the source spectrum. It is noted at this point that we cannot exclude the possibility of some contami-

[2] Following broad-band AAT spectroscopy (3400–10,000 Å) on 1986 February 7, we have identified EXO 054147−4049.5 with a $V \approx 17.2$ QSO showing a single prominent and broad line at a wavelength of 7215 Å. If this line is Mg II λ2796, the implied redshift is $z = 1.58$.

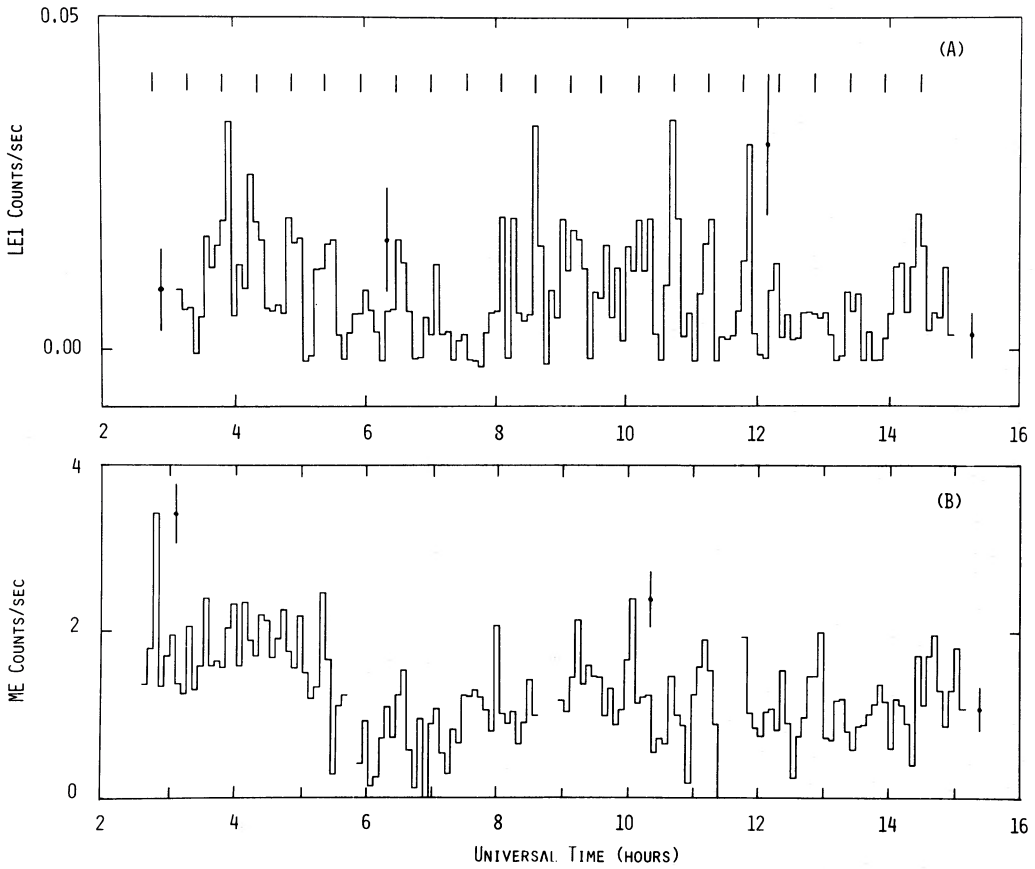

FIG. 5.—*EXOSAT* time series for 1H 0542−407 on 1985 February 23 obtained using LE1 (*a*) and the ME (*b*). The data have been binned into 300 s samples and representative $\pm 1\ \sigma$ error bars are shown. Individual pulsations corresponding to the 1920 s periodicity (see text) are marked for the LE1 data. Note the amplitude modulation of the pulsations at a period near 6.2 hr.

nation in both these sets of ME data from EXO 054147−4049.5 lying 13′.6 away from the cataclysmic variable. If both sources have similar spectra, the contamination at most would be 21% (allowing for the reduced collimator response and the lower intensity of EXO 054147−4049.5).

Figure 5*b* shows the ME time series data between 1 and 9 keV. The ME data were folded over the same total period range as LE1, and the resulting χ^2 versus period plot for the interval 1500–2500 s is shown in Figure 6*b*. Two peaks are evident once again. The first is consistent with the 1920 s periodicity determined more precisely by the LE1 data, while the second peak, which is more pronounced in the ME data, has a centroid of 2120 ± 30 s. The ME light curve corresponding to the 1920 s periodicity is depicted in Figure 7*b*. The pulse fraction is $\sim 20\%$ semiamplitude.

The light curves for the 1920 s periodicity in the LE1 and ME data (Fig. 7) are closely aligned in phase. However, the hard X-ray light curve is less sinusoidal, with a sharp and narrow minimum centered on the soft X-ray minimum. We calculate a time reference for X-ray maximum, based on the folded LE1 data, of HJD $2{,}446{,}119.5917 \pm 0.0021$.

Both the LE1 and ME data show clear evidence for a second and longer periodicity. The centroid periods inferred from the two instruments differ by ~ 40 s, but are consistent with a mean value of 2100 ± 20 s. The close proximity of this second period to the pronounced 1920 s modulation is very suggestive of a beat phenomenon involving a much longer period of 6.2 ± 0.5 hr. Amplitude modulation of the individual LE1 pulsations over nearly two ~ 6.2 hr cycles can in fact be discerned in Figure 5*a* and accounts for the pulse variability noted earlier. The modulation semiamplitude for the ~ 6.2 hr periodicity is roughly 65% with a maximum at HJD $2{,}446{,}119.67 \pm 0.02$. We note that the ME light curve (Fig. 5*b*) also shows evidence for the 6.2 hr periodicity, particularly the first cycle where the maximum and minimum are approximately coincident with those of the LE1 data. The ~ 6.2 hr modulation semiamplitude in the ME data appears comparable to that of the LE1 light curve in the first cycle but is evidently less during the second cycle. In summary, we conclude that an underlying periodicity of ~ 6.2 hr is present in 1H 0542−407, in addition to the pulsation period of ~ 1920 s.

We have performed a cross-correlation analysis of the LE1 and ME data for 1H 0542−407. The two data sets were first co-aligned by binning the 10 s samples into successive intervals during the LE1/ME overlap period between 3.2 and 14.9 UT. Binning intervals of 100 s and 400 s were used, and a few missing samples were padded with the local mean. The data were then detrended using a third-order polynomial before computing the partially unbiased cross-correlation functions according to the prescription of Stella, Kahn, and Grindlay (1984). The resulting functions are shown in Figures 8*a* and 8*b* for short and long lag time scales corresponding to the 100 s and 400 s binning times. The low- and medium-energy data show a strong correlation approaching 100% for time lags

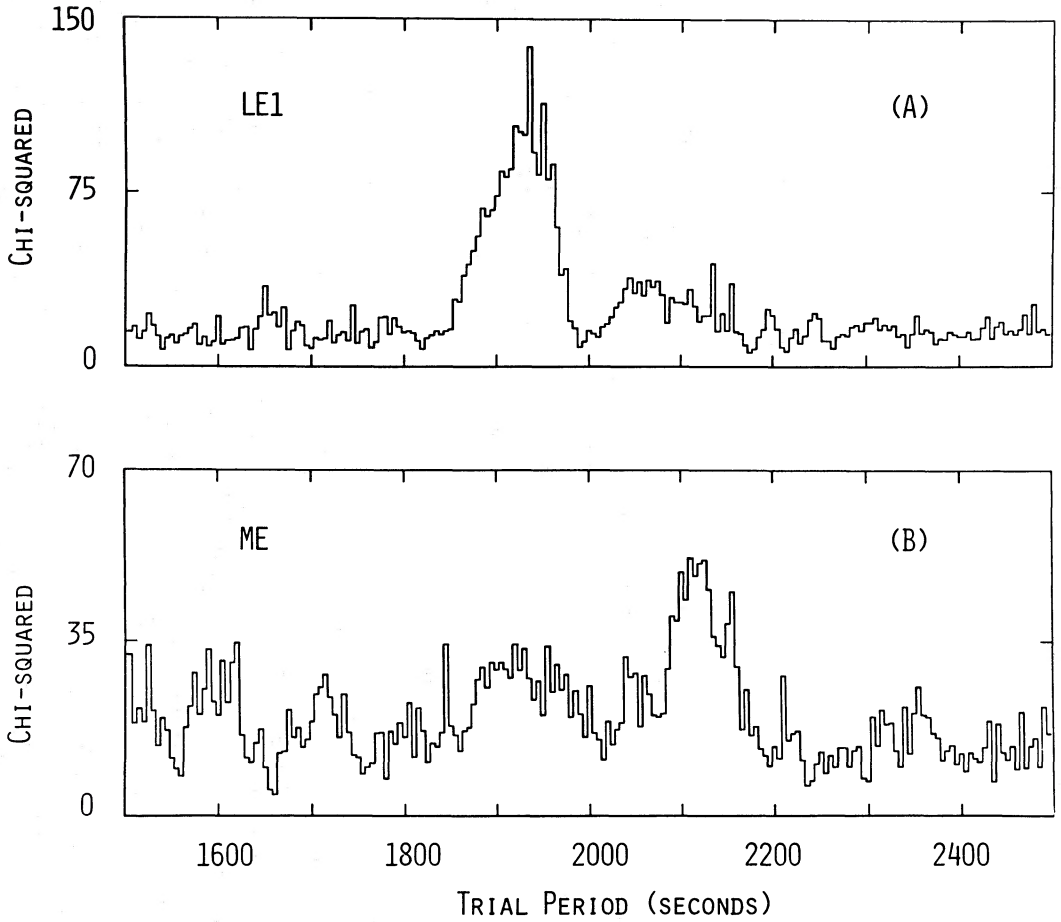

FIG. 6.—Chi-squared for 16 phase bins vs. trial period for the *EXOSAT* observation of 1H 0542−407. Two periodicities are evident in both the LE1 (*a*) and ME (*b*) data. Centroid values are 1920 s (LE1 and ME), 2084 s (LE1), and 2120 s (ME). Note that the shorter period is more pronounced than the longer period in the LE1 data, whereas the converse is true for the ME data.

$\lesssim$200 s. Both figures show multiple peaks corresponding to the $\sim$1920 s periodicity, while the effect of the $\sim$6.2 hr modulation is apparent in Figure 8*b*. Figure 8*a* also shows evidence for a time asymmetry in the sense that the low-energy 1920 s pulsations lag those in the medium-energy band. Alternately, this asymmetry may well be a consequence of the differing pulse profiles in the LE1 and ME energy ranges (Figs. 7*a* and 7*b*).

c) 1H 0542−407 X-Ray Spectrum

The total ME observation of 1H 0542−407 provided high signal-to-noise ratio spectral data in the energy range 1.2–9.3 keV. These spectral channels, together with the single broad-band (0.1–1.0 keV) LE1 data point, were fitted with both power-law and thermal bremsstrahlung spectra, each with interstellar absorption. The resulting parameters and chi-squared values are summarized in Table 2, and the fitted power-law spectrum is plotted in Figure 9. The spectrum is clearly very hard. In fact, for a thermal model, the lowest values of χ^2 were obtained for unbounded values of kT well above our energy range. We therefore quote a 90% confidence lower limit on kT of 10 keV. The interstellar absorption measured for both models is $\sim 1 \times 10^{21}$ cm^{-2} but is consistent with zero at the 90% confidence extreme.

Both the power-law and thermal spectra gave statistically acceptable fits to the combined LE1/ME data. Inspection of the residuals, however, indicated a local enhancement near the expected position of an iron emission line at $\sim$6.7 keV. Accordingly, an iron line of narrow width and fixed energy of 6.7 keV was added to the model spectrum to characterize this feature. A reduction in chi-squared from $\chi^2 = 20.6$ ($\nu = 23$) to $\chi^2 = 15.2$ ($\nu = 22$) was achieved for a best-fit equivalent width of 0.40 keV. We therefore believe that the feature, which corresponds to a 3–4 σ enhancement relative to the local continuum, is a real iron line.

Using the best-fit parameters given in Table 2, we derive the following time-averaged fluxes for 1H 0542−407: 7.6×10^{-12} ergs cm^{-2} s^{-1} (0.1–2 keV) and 3.3×10^{-11} ergs cm^{-2} s^{-1} (2–10 keV). The average 2–10 keV flux is $\sim$50% higher than that measured in 1977–1979 by *HEAO 1* (§ II*a*).

d) H0534−581 X-Ray Image

An X-ray image of the H0534−581 field was obtained with LE1 between 1025 and 1851 UT on 1984 November 18 using the 3000 Lexan filter. A single point X-ray source with an intensity of 0.0252 ± 0.0012 counts s^{-1} was detected near the center of the field at a position of $\alpha = 05^h34^m02^s.3$, $\delta = -58°03'31''.8$ (1950). This position lies only 1″ from our AAT position for the cataclysmic variable (§ II*b*), thereby confirming our identification of the *HEAO 1* X-ray source. No other X-ray sources were found in the $\sim$1°.5 field.

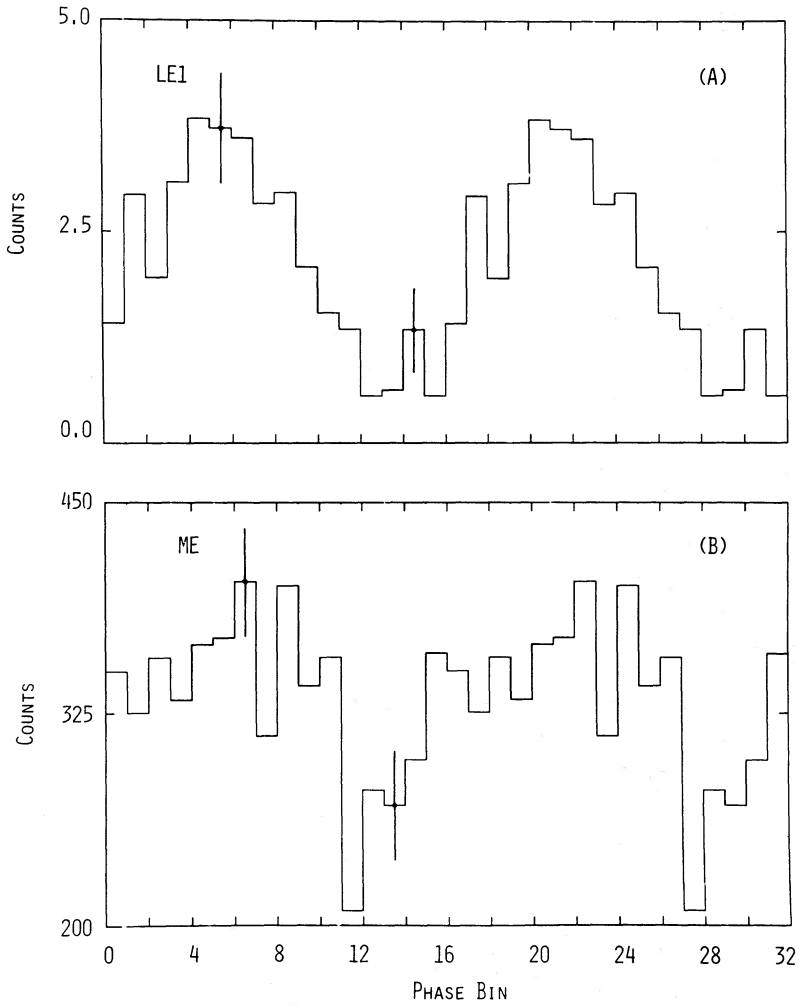

FIG. 7.—Folded and background-subtracted 1920 s light curves for the *EXOSAT* observation of 1H 0542−407 on 1985 February 23. The data for LE1 (0.1–1 keV) are shown in (*a*), and for the ME (1–9 keV) in (*b*). Both light curves are plotted twice for clarity, and representative $\pm 1\ \sigma$ error bars are shown. The beginning of each light curve corresponds to 0200 UT.

e) H0534−581 Time Series Analysis

LE1 time series data with a sample time of 10 s were derived from the H0534−581 image data in a manner identical to that described for 1H 0542−407. Accompanying ME data were also acquired between 1005 and 1857 UT. Swapping of the ME array halves (H1 and H2) to measure the background separately in each array was not possible during the H0534−581 observation. However, the on-source measurement by H1 was preceded by an 80 minute spacecraft slew, which provided clean and simultaneous measurements of the background spectra in both array halves. A "difference spectrum" between these two data sets was used to calculate the background in H1 throughout the H0534−581 measurement from the background countrate in the offset H2 array. In this way, both a time series file of 10 s samples, and an X-ray spectrum were produced. The LE1 and ME light curves are plotted in Figures 10*a* and 10*b* (discussed later).

TABLE 2

EXOSAT SPECTRAL PARAMETERS

Source	Normalization	α or kT	$N_H(10^{20}\ \mathrm{cm}^{-2})$	χ^2	ν
1H 0542−407:					
Power Law	0.0039 ± 0.0002	1.24 ± 0.3	10^{-10}_{+30}	20.6	23
Thermal Bremsstrahlung	...	≥ 10	10^{-10}_{+30}	20.2	23
H0534−581:					
Power Law	0.0018 ± 0.0001	$0.87^{-0.02}_{+0.05}$	$0.1^{-0.1}_{+5.0}$	28.0	23
Thermal Bremsstrahlung	...	≥ 30 keV	$0.1^{-0.1}_{+5.0}$	42.7	23

NOTES.—Errors on parameters and lower limits on kT are 90% confidence. α is a power-law photon index.

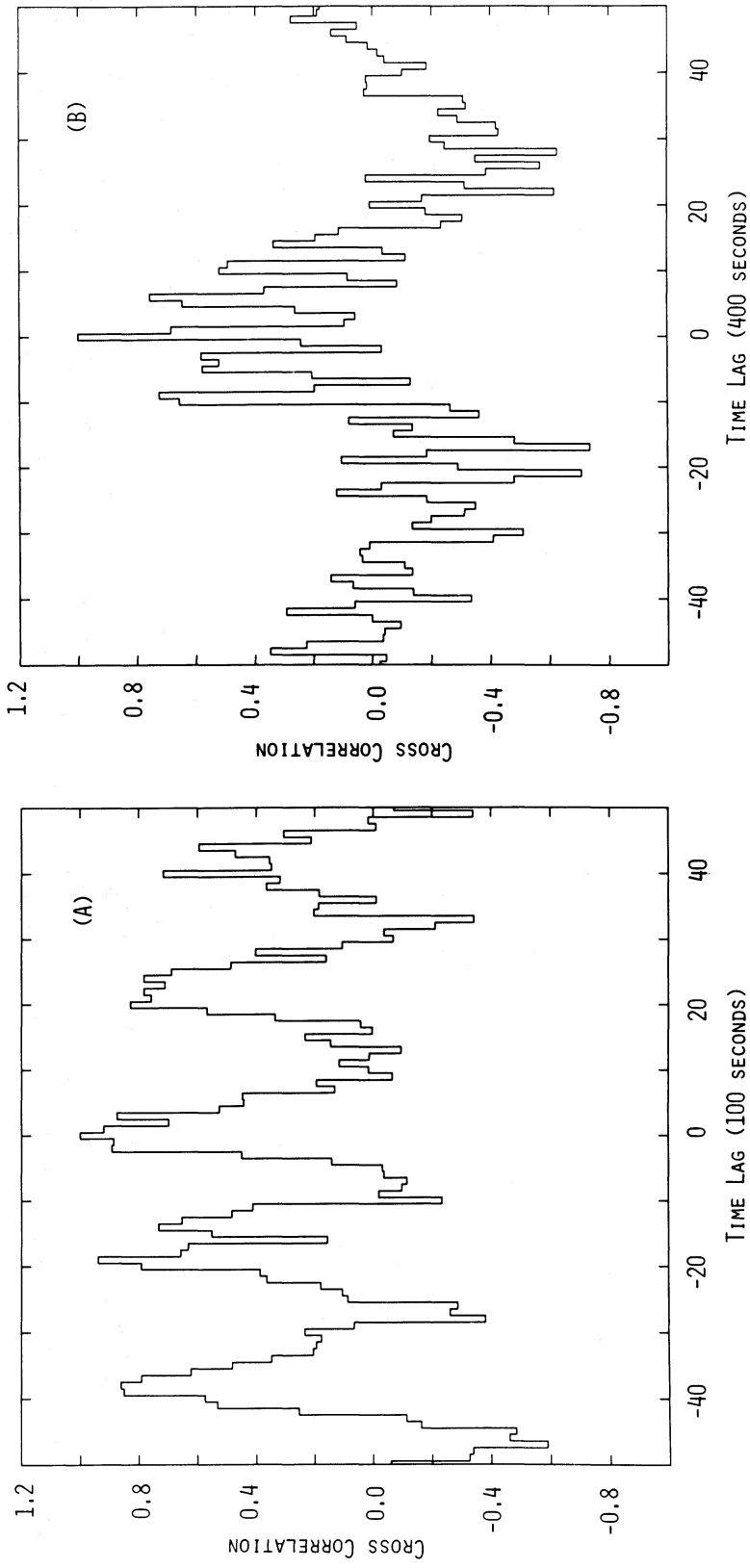

FIG. 8.—Cross-correlation analysis for the *EXOSAT* LE1 and ME observations of 1H 0542−407. The results for a data binning time of 100 s and a total lag of ±5000 s are shown in (*a*), and for a binning time of 400 s and a total lag of ±20,000 s in (*b*). Multiple peaks due to the 1920 s X-ray pulsations are evident in both plots.

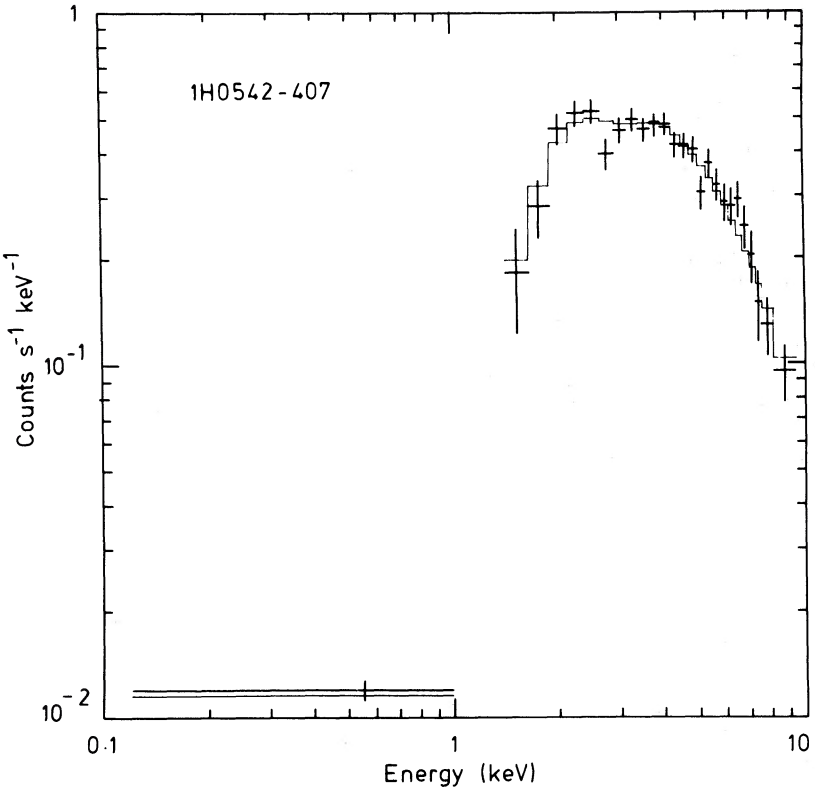

FIG. 9.—Power-law spectrum fitted to the 1H 0542−407 LE1 and ME data obtained by *EXOSAT* (see Table 2). A 3–4 σ excess relative to the local continuum data is evident at the expected position of a 6.7 keV iron line.

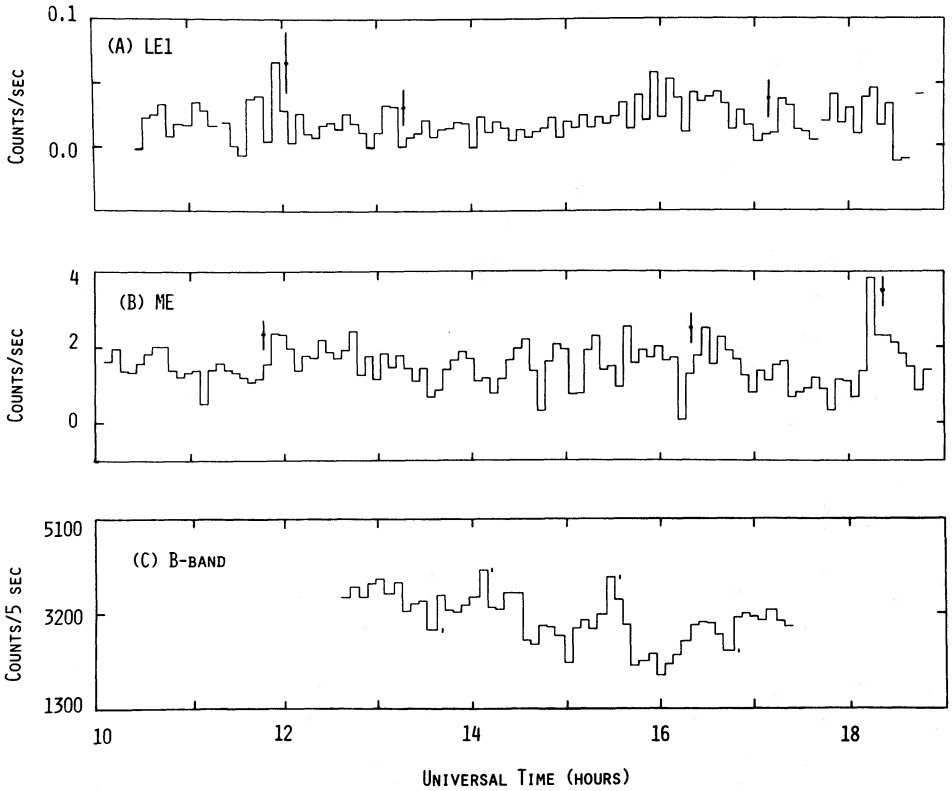

FIG. 10.—Intensity data for H0534−581 on 1984 November 18. The plots show *EXOSAT* 0.1–1 keV LE1 (*a*) and 1–9 keV ME (*b*) data, together with overlapping *B* band photometry (*c*). All data have been binned into ~300 s samples. Representative ± 1 σ error bars are plotted.

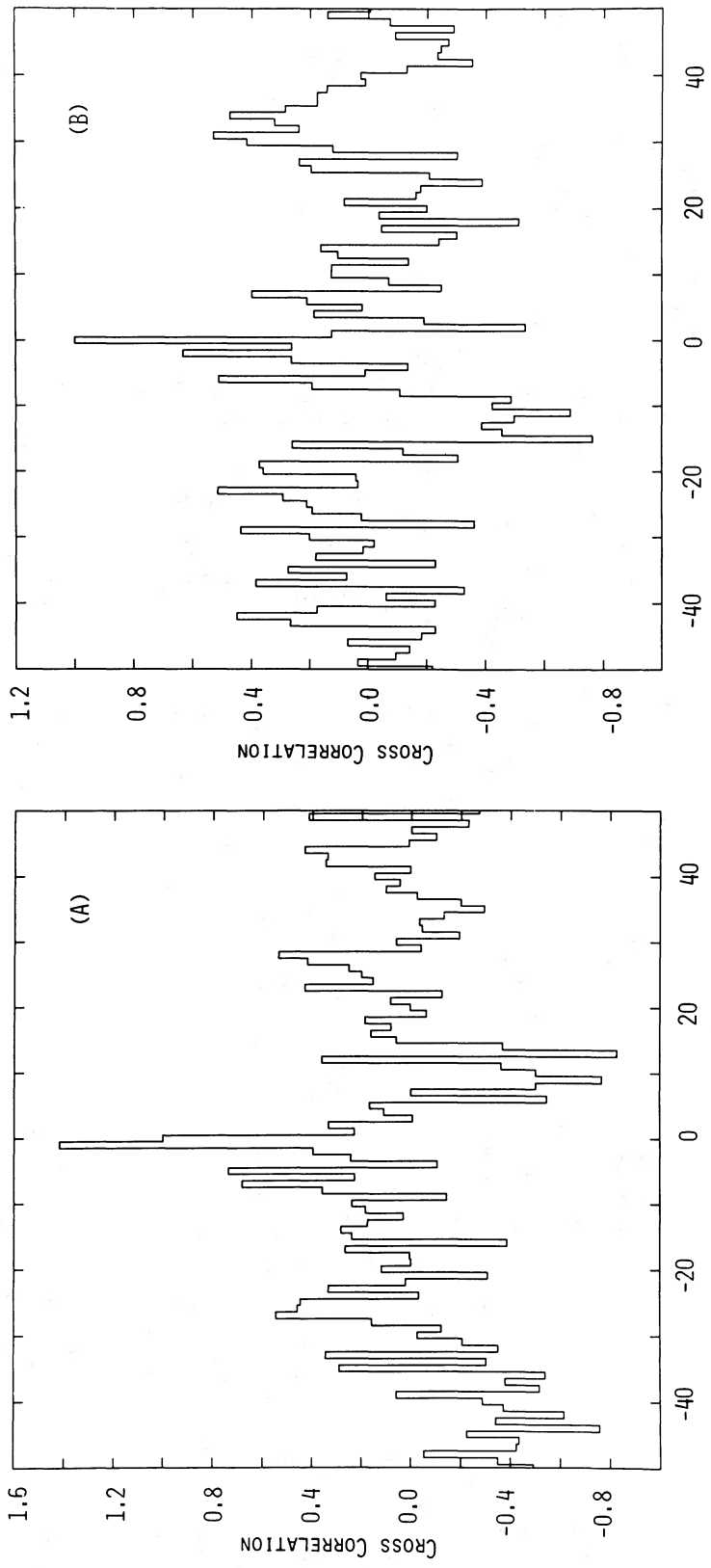

FIG. 11.—Cross-correlation analysis for the *EXOSAT* LE1 and ME observations of H0534−581. The two plots show the results for a binning time of 100 s and a total lag of ±5000 s (*a*), and for a binning time of 400 s and a total lag of ±20,000 s (*b*).

A search for periodic behavior was made by folding the LE1 and ME data at trial periods ranging from 100 to 10,000 s. No dominant χ^2 peak analogous to that for 1H 0542−407 was found in either data set. Smaller χ^2 peaks were evident, but none are common to both LE1 and the ME. These peaks occur at 5015 ± 40 s, 5610 ± 50 s, 7550 ± 30 s, and 8470 ± 100 s in LE1, and at 1325 ± 25 s, 2315 ± 30 s, 2670 ± 40 s, and 4610 ± 100 s in the ME. With the possible exception of the 1325/2670 s and 2315/4610 s peaks, none of the folded light curves for these periods appears plausible, and thus it is likely that they are artifacts resulting from statistical fluctuations in the data. In any event, we have determined upper limits for periodic X-ray emission by injecting sinusoidal signals into the LE1 and ME data. The limits at representative periods between 100 and 10,000 s are summarized in Table 3 and correspond to a pulse fraction which produces a distinct χ^2 peak comparable to those noted in the analysis above.

A cross-correlation analysis of the overlapping LE1 and ME data between 10.5 and 18.7 hours UT was undertaken for H0534−581 using an identical procedure to that described for 1H 0542−407. Figures 11*a* and 11*b* show the cross correlation functions for short and long lag ranges corresponding to data binning times of 100 s and 400 s. The low-energy and medium-energy data exhibit a significant degree of correlation over a short time lag of $\lesssim$100 s. No correlation on longer time scales is evident, with the possible exception of a broad peak in Figure 11*b* at a positive lag time of ~3.6 hr. It seems unlikely, however, that this feature has real physical significance (e.g., an orbital period) since a corresponding peak is not present at a negative time lag.

The *EXOSAT* observation of H0534−581 coincided with successful photometry of the optical counterpart from Siding Spring Observatory (§ IV*c*). The *B* band count rate (cf. Fig. 15*c*) has been summed into 300 s bins to match the X-ray data and is plotted in Figure 10*c*. Variability is evident in the X-ray data, but the low count rate and the absence of periodic emission makes an investigation of correlated optical behavior difficult. Nevertheless, it is clear that no substantial correlation between the X-ray and optical data is present. For instance, the decline of ~40% in the mean *B* band flux between 1230 and 1500 is not evident in either the LE1 or ME light curves, which remain constant to <20%. Similarly, the ~80% flare in the *B* band flux at 1530 is not present in the LE1 data (constant to <20%). An increase in the ME count rate is indicated during the optical flare, but the respective maxima are displaced by ~10 minutes. We conclude from our simultaneous observations that the X-ray and optical fluxes from H0534−581 do not show a consistent correlation to within at least a factor of 2 on a time scale of order 10–60 minutes. We also note from the X-ray data of Figure 10 that there is no clear indication of an orbital period on a time scale of 1–4 hr.

TABLE 3

UPPER LIMITS ON PERIODIC X-RAY EMISSION FROM H0534−581

Period (s)	LE1 (0.1–1 keV)	ME (1–9 keV)
100.....	25%	20%
1000.....	30%	20%
10000.....	40%	30%

NOTE.—Upper limits are semiamplitude pulse fractions derived assuming sinusoidal modulation.

f) H0534−581 X-Ray Spectrum

The ME spectral data for H0534−581, supplemented by the 0.1–1 keV LE1 data point, were modeled in a manner similar to that described for 1H 0542−407. Table 2 summarizes the least-squares spectral parameters and chi-squared values for power-law and thermal models. The power-law fit, which gave a significantly lower value of chi-squared, is shown in Figure 12. An exceedingly hard spectrum is indicated, together with low absorption. Although the power-law fit is quite acceptable, there is a ~2 σ positive deviation in the residuals near 6.7 keV. We do not claim detection of an iron line, but if this enhancement is real, it corresponds to an equivalent width of ~0.4 keV.

Broad-band fluxes for H0534−581 corresponding to the power-law parameters in Table 2 are as follows: 5.4×10^{-12} ergs cm^{-2} s^{-1} (0.1–2 keV) and 2.9×10^{-11} ergs cm^{-2} s^{-1} (2–10 keV). The 2–10 keV flux is almost identical to that measured by *HEAO 1* in 1977–1979 (§ II*b*).

IV. OPTICAL PHOTOMETRY

a) Instrumentation

Optical photometry of the two cataclysmic variables was undertaken using the Two Channel Chopper (TCC) at the Cassegrain focus of the 1.0 m telescope at Siding Spring Observatory (SSO). Additional data were also obtained during a commissioning run on the new 2.3 m telescope at SSO. On this occasion, the TCC was mounted at one of the two Nasmyth focii of the alt-az telescope.

A full description of the TCC will be given by Bessell (1986). Briefly, the instrument has eight selectable pairs of star/sky apertures which are separated by 141″ (1.0 m) and 61″ (2.3 m). A four-sector chopper rotating at 18 Hz deflects the light beams from the pair of apertures into two independent filter/photomultiplier units in such a way that each photomultiplier samples both the star and the sky apertures alternately. Control of the instrument, including the two filter wheels, is by a PDP11 computer. A menu of data acquisition programs can be constructed to define repetitive observation cycles consisting of successive filter pairs and integration times.

For example, our acquisition cycle for measuring standard stars (Graham 1982; Landolt 1983) at the beginning and end of each night consisted of a sequence of five filter pairs, with the same filter being measured simultaneously in GaAs and S20 photomultipliers; i.e., *U*: *U*(10), *B*: *B*(5), *V*: *V*(5), *R*: *R*(5). *I*: *I*(5), where the numbers in parentheses were the effective integration times in seconds for each tube. Because the two tubes are selected alternately by the chopper, the *elapsed* time to complete a pair of measurements was double the times shown, plus a small overhead factor.

The TCC measurements of 1H 0542−407 and H0534−581 were conducted in an identical configuration for each object. A TCC acquisition cycle for the GaAs and S20 photomultipliers was defined as follows:— *B*: *B*(5), *U*: *B*(10), *B*: *V*(5), *V*: *R*(5), *R*: *I*(5). This program had several advantages. First, the simultaneous pair of *B* measurements at the start of each cycle provided continual cross-calibration between the two photomultipliers. Second, the remaining four pairs of measurements in adjacent filters for the two tubes permitted $U-B$, $B-V$, $V-R$, and $R-I$ to be determined on a *simultaneous*

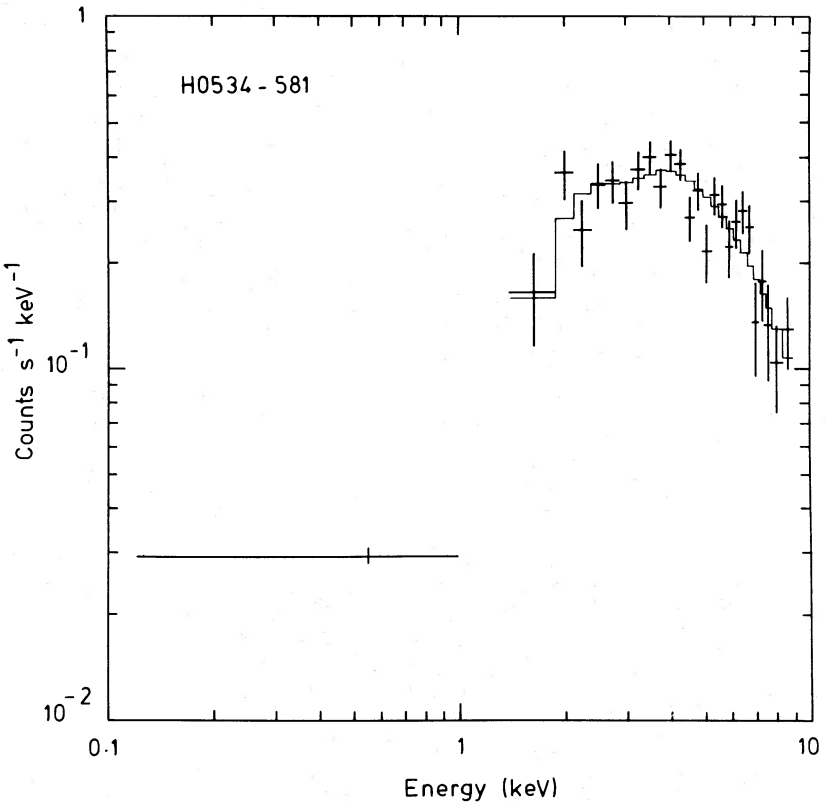

FIG. 12.—Power-law spectrum fitted to the H0534 − 581 LE1 and ME data obtained by *EXOSAT* (see Table 2)

basis (i.e., rather than by measuring filter pairs sequentially in time). This feature of the TCC is particularly useful for the study of cataclysmic variables where significant intensity variations can occur in a time scale of seconds. Third, the relative phasing of the *B* measurements on the GaAs tube provided data in this filter at double the frequency available for the four colors. Specifically, the time between successive 5 s *B* measurements was ~40 s, compared with an overall cycle time of ~80 s between color measurements. Note that these times include overheads of ~10 s and ~20 s, respectively, corresponding to filter movements and data recording. This deadtime is slightly variable, and thus the data points are not precisely equispaced.

b) 1H 0542−407

1H 0542−407 was observed with the TCC on 1984 November 20, November 21, and 1985 January 20 under conditions of 1″–3″ seeing. It was not possible to exclude light from the neighboring star ~3″ to the west of 1H 0542−407 (§ II*a*), so both stars were always within the TCC aperture (14″ or 17″ diameter). The *B* light curves and colors for the three observations are shown in Figure 13. Photometric variability over a range $\Delta B \approx 1.2$ mag can clearly be attributed to the cataclysmic variable. The average *V* magnitude and typical colors for *both* stars together are as follows: $V \approx 14.9$, $U-B \approx -0.95$, $B-V \approx +0.3$, $V-R \approx +0.4$, and $R-I \approx +0.3$.

We are able to approximately derive the intrinsic magnitudes and colors of 1H 0542−407 from our photometry with the aid of the AAT spectrum of the contaminating star (§ II*b*). By assuming that the light loss at the spectrograph slit at a particular wavelength affected both stars equally, and by determining relative intensities for *U*, *B*, *V*, and *R* from the spectra, we deduce the average *V* magnitudes and colors shown in Table 4. We note that the observed variability of $\Delta B \approx 1.2$ mag corresponds to an intrinsic variability of $\Delta B \approx 1.6$ mag in the

TABLE 4

OPTICAL PHOTOMETRY

	1H 0542−407[a]		H0534−581
MAGNITUDE	Cataclysmic Variable	Adjacent Star	Cataclysmic Variable
V	~15.7	~15.6	~14.9
U−*B*	−1.2 ± 0.2	+0.32 ± 0.3	−1.15 ± 0.05
B−*V*	−0.2 ± 0.2	+0.93 ± 0.2	−0.2 ± 0.1
V−*R*	+0.2 ± 0.2	+0.52 ± 0.2	+0.1 ± 0.1
R−*I*	...	...	+0.1 ± 0.2

[a] Average *V* magnitudes and colors for both stars were deduced using the procedure discussed in the text.

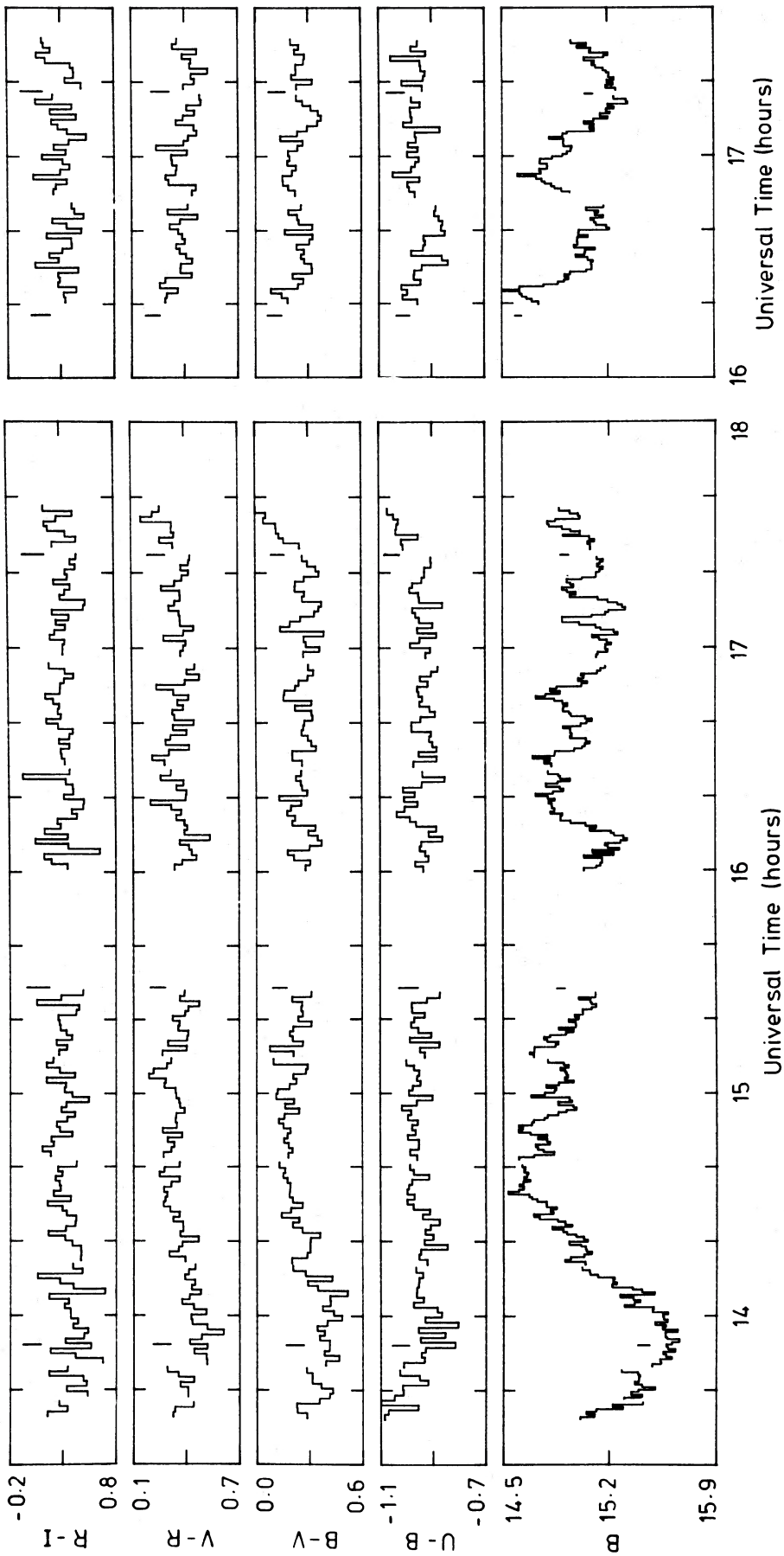

FIG. 13*b*

FIG. 13.—TCC photometry of 1H 0542−407 *and* the adjacent star for 1984 November 20 (*a*), November 21 (*b*), and 1985 January 20 (*c*). The November data were obtained using the 1.0 m telescope, while the January measurements were made with the new 2.3 m telescope at SSO. Data points in the *B* light curves are ~40 s apart, compared with ~80 s for the color measurements. The vertical lines represent $\pm 1\sigma$ Poisson error bars.

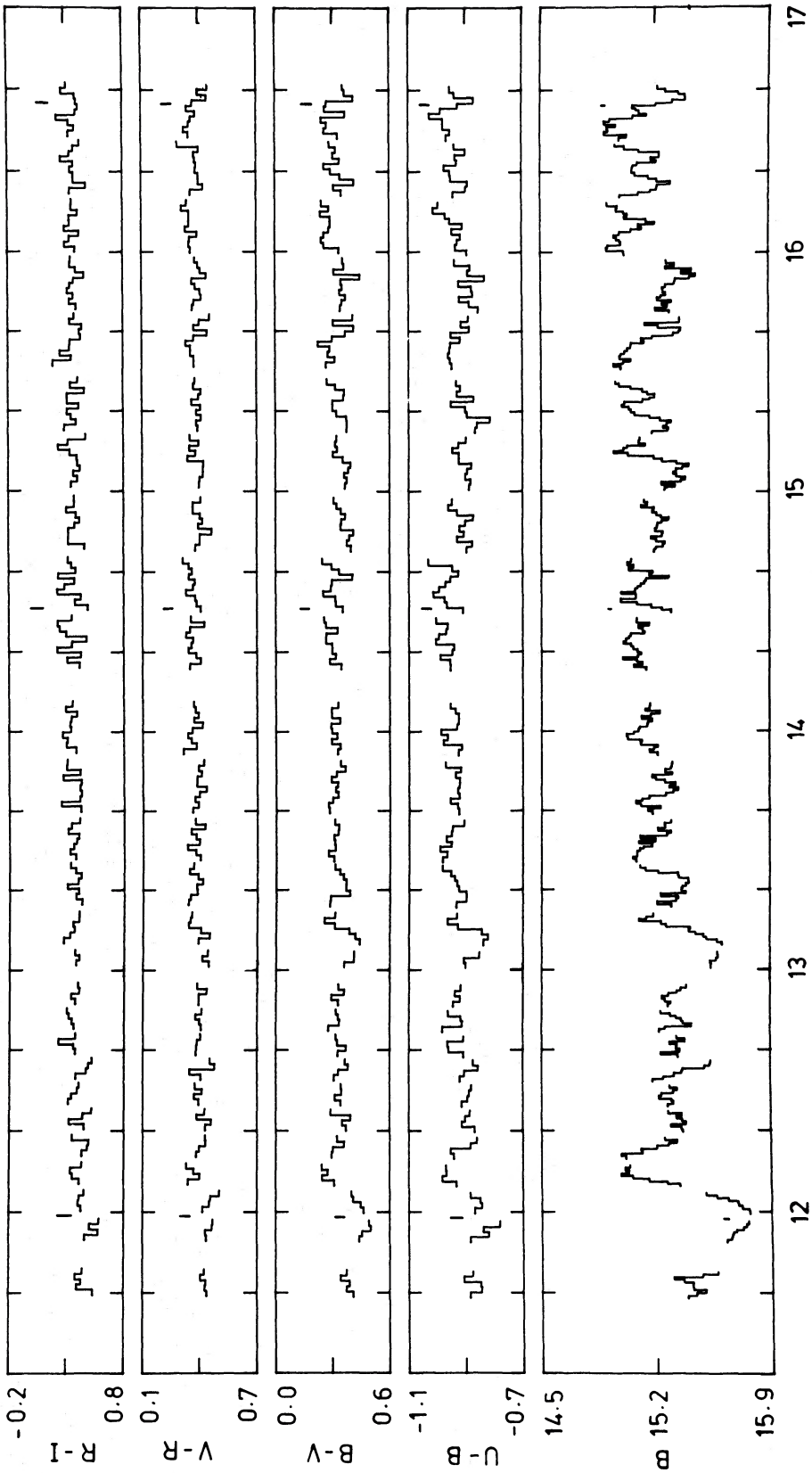

FIG. 13c

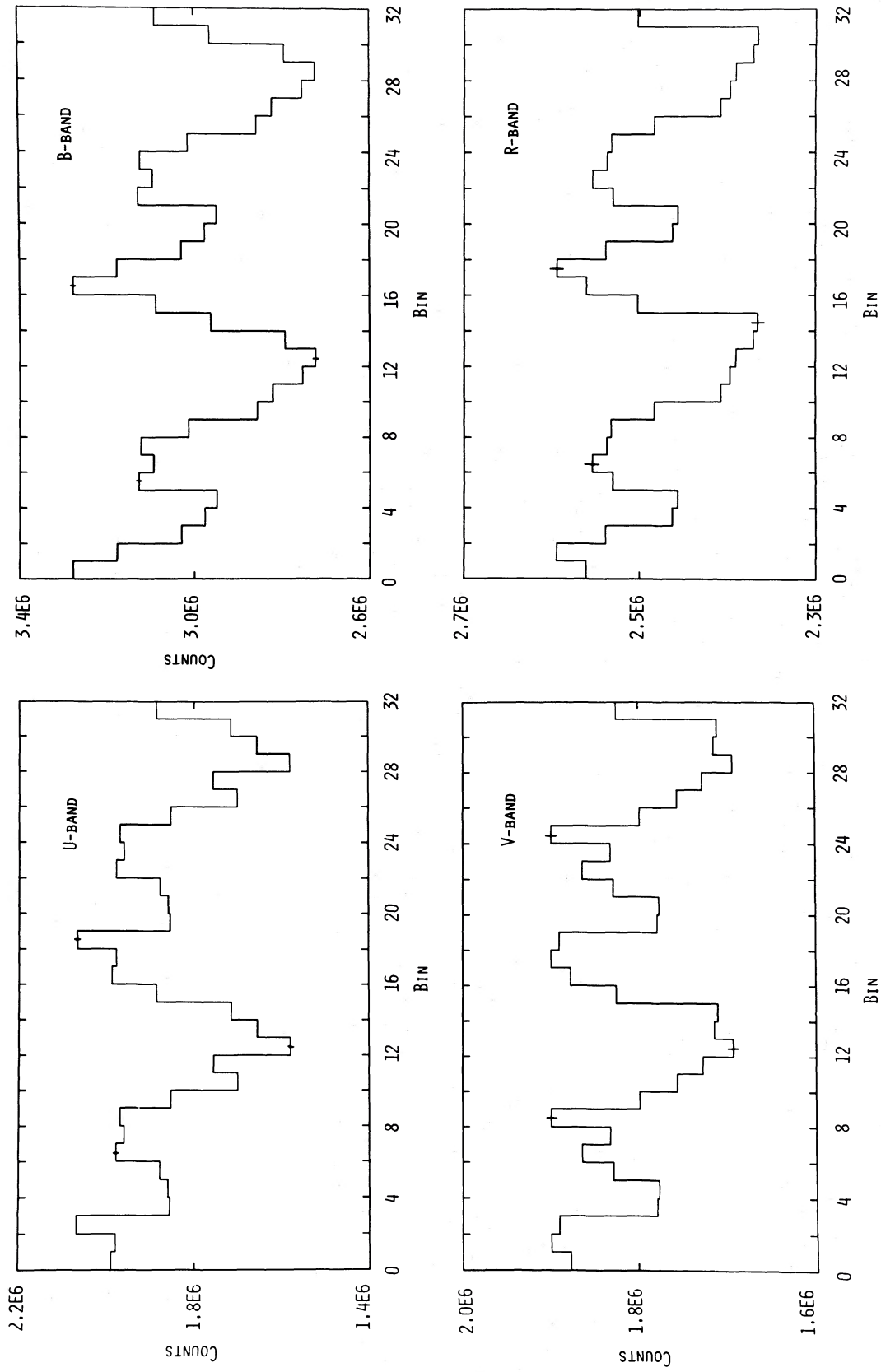

FIG. 14.—*U*, *B*, *V*, and *R* light curves for 1H 0542 − 407 on 1985 January 20 folded at a period of 1980 s. The time reference for the start of the first bin is 1100 UT. The data are folded twice for clarity, and representative $\pm 1\,\sigma$ error bars are plotted.

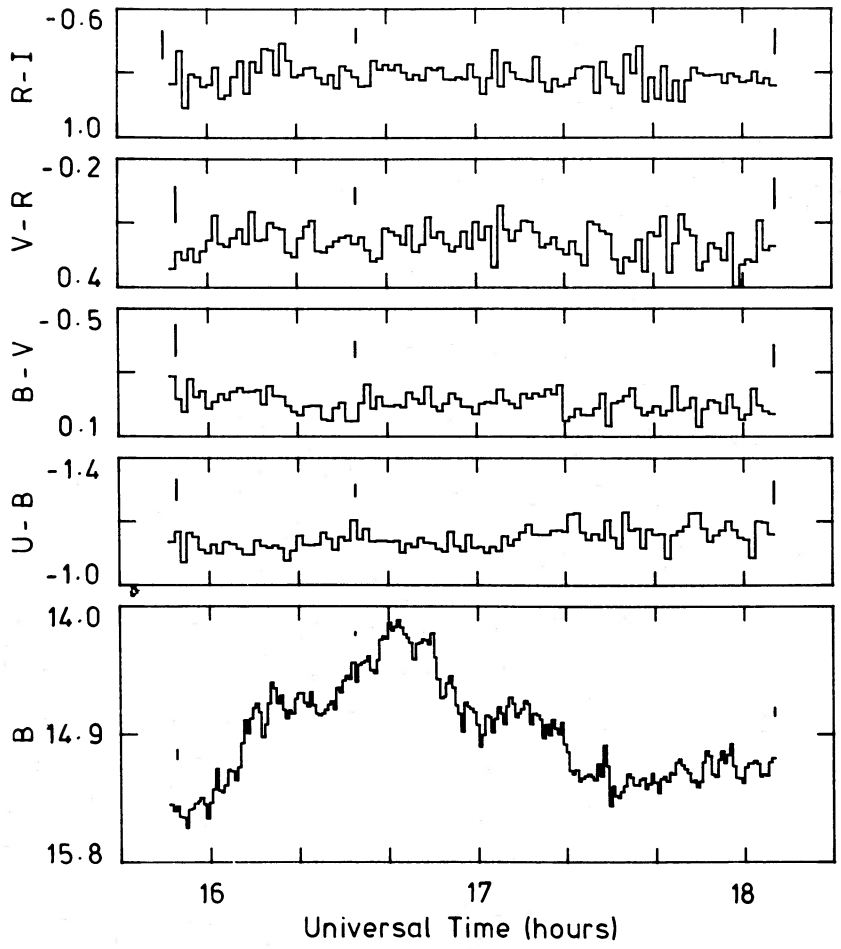

FIG. 15*a*

FIG. 15.—TCC photometry of H0534−581 obtained on 1984 October 24 (*a*), November 17 (*b*), and November 18 (*c*) using the 1.0 m telescope at SSO. The photometry of November 18 was partly simultaneous with *EXOSAT* data (Fig. 10). Time resolution and error bars are the same as Fig. 13.

cataclysmic variable, and that the colors for the adjacent star are consistent with our spectral classification of this object (§ II*a*).

Flickering behavior from 1H 0542−407 is present in the light curves of Figure 13 on time scales ranging upward from our sampling time of 40 s. The correlated changes in the color indices that can be seen are due to the increasing proportion of blue light to the total signal from the two stars as 1H 0542−407 becomes brighter (i.e., the color variation is an artifact). In view of the contamination caused by the adjacent star, we cannot comment reliably on any intrinsic color variability in the cataclysmic variable.

The TCC data for 1H 0542−407 have been examined for periodic behavior using an epoch-folding technique similar to that applied to the X-ray data (§ III). The *B* band data sampled every ∼40 s were used for this analysis. For the ∼3 hr and ∼5 hr runs on 1984 November 20 and 1985 January 20, broad χ^2 peaks at periods of 2015^{+50}_{-150} s and 1980 ± 35 s, respectively, were found. A similar periodicity is indicated by the ∼1970 s separation between the two pronounced maxima observed during the short observation of 1984 November 21 (Fig. 13*b*). From our three independent observations we therefore infer that modulation at a centroid period of 1980 ± 35 s is a persistent feature of the optical emission from 1H 0542−407. This periodicity is intermediate between the 1920 s and ∼2100 s periods found in the X-ray data (§ III). We point out that χ^2 peaks at other periods were also present for the two long optical observations, but since these periods are not common to both runs and do not have analogs in the X-ray data, we conclude that they are artifacts of the flickering behavior.

The *U*, *B*, *V*, and *R* light curves folded at a period of 1980 s are shown in Figure 14 for the 5 hr observation of 1985 January 20. The semiamplitude pulse fractions, corrected for the estimated contamination from the neighboring star, are ∼14%, ∼12%, ∼11%, and ∼11%, respectively, i.e., there is no significant color dependence of the pulse fraction. All four light curves are similar in appearance, showing both primary and secondary peaks separated by ∼740 s. Folding of our multicolor photometry of 1984 November 20 and 21 produced light curves comparable to those in Figure 14. Maximum light for the primary peak in our three observations occurred at HJD 2,446,025.1088 ± 0.0014, HJD 2,446,026.1851 ± 0.0014, and HJD 2,446,085.9613 ± 0.0014.

c) H0534−581

H0534−581 was observed on 1984 October 24, November 17, and November 18. The seeing was in the range 1″–3″, and a TCC aperture of 14″ diameter was used. The resulting *B* light

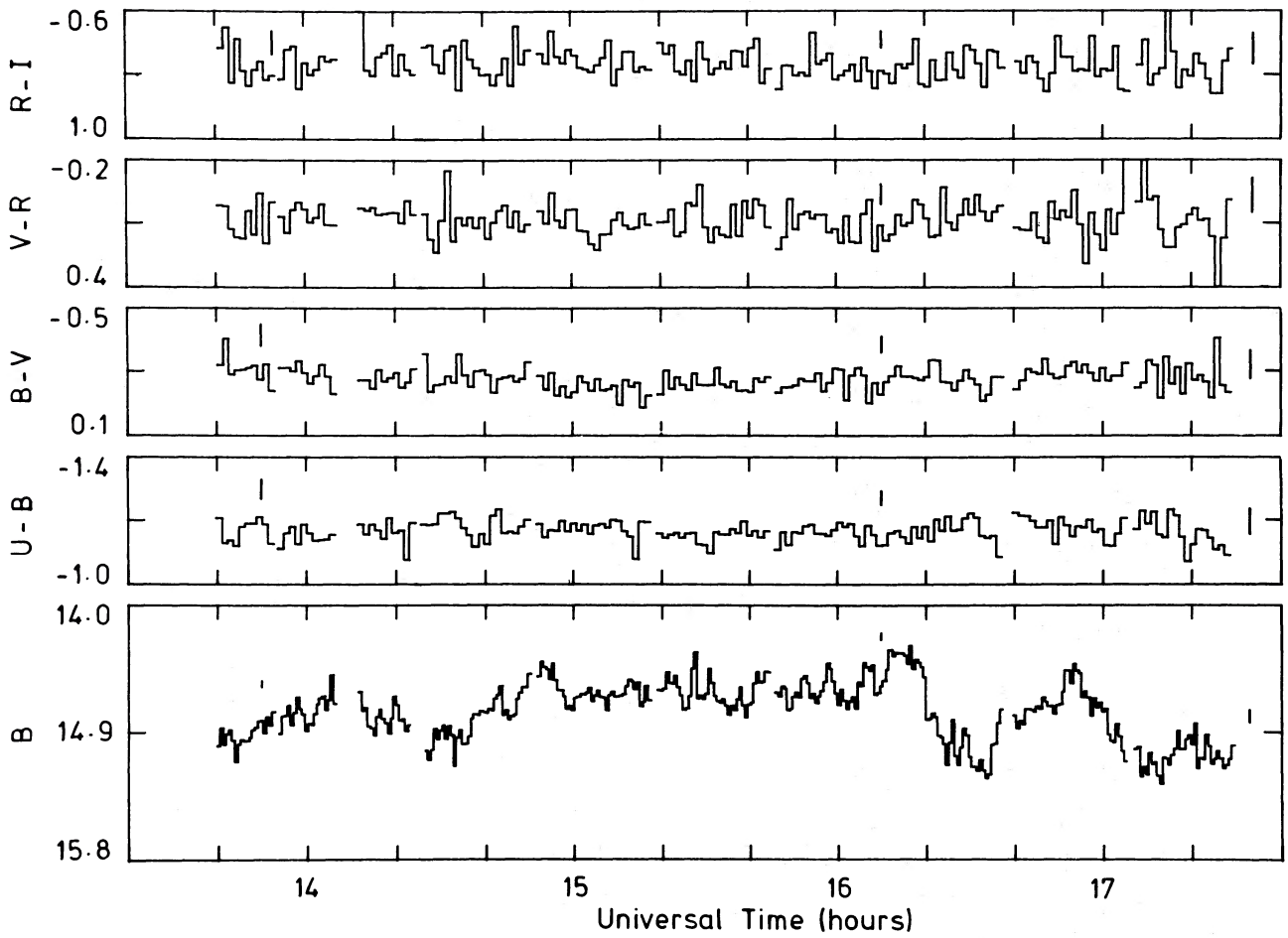

FIG. 15*b*

curves and simultaneous $U-B$, $B-V$, $V-R$, and $R-I$ colors are plotted in Figure 15. The B magnitude varies over a range of 15.6–14.1 mag. Average V magnitude and colors for H0534−581 are summarized in Table 4.

Significant flickering from H0534−581 is evident in the light curves (Fig. 15) on time scales ranging from our sampling interval of 40 s to many minutes. These intensity variations are not accompanied by substantial changes in the color indices. A correlation analysis confirms that there is no systematic relationship between B and $U-B$, or B and $B-V$. However, the mean colors do vary between our three runs in the sense that the star becomes bluer with time ($B-V$ decreases by ~ 0.2 mag). Smaller variations in the average colors can also be seen within a run; e.g., $U-B$ decreases by ~ 0.04 mag in the latter half of Figure 15*a*.

The B band TCC data having a sample time of ~ 40 s were folded to search for periodicities between 400 and 3000 s. Prominent χ^2 peaks were found at several trial periods for the three runs: 1770^{-50}_{+100} s (October 24), 1915 ± 40 s (November 17), 2550 ± 70 s (November 17), 1275 ± 35 s (November 17), 2540 ± 50 s (November 18), and 3020 ± 50 s (November 18). All of these possible periods produce plausible light curves. However, none of the periods are common to all three runs, or to any of the possible periods found in the X-ray data (§ III*d*). The periodicity corresponding to 1275/2550 s is nevertheless of interest because it is present in the data from the two consecutive nights in November. The modulation semiamplitudes in the B band light curves are as follows: $\sim 16\%$ (2550 s, November 17), $\sim 9\%$ (1275 s, November 18), and $\sim 13\%$ (2550 s, November 18; two peaks of unequal amplitude). Further photometry is needed to determine whether this periodicity occurs regularly in the optical emission from H0534−581 and thus has real physical significance.

We are unable to discern a repeatable orbital period on a time scale of <4 hr in our three observations of H0534−581 (Fig. 15). The short observation of October 24 cannot be reconciled with either of the longer observations on the two consecutive nights in November. For the latter two runs there is a degree of similarity when the light curves are aligned with a separation of ~ 23.2 hr. This could be consistent with a possible period of $\sim 23.2/n$ hr, where $n < 6$.

IV. DISCUSSION

Our *EXOSAT* observations of the two cataclysmic variables leave no doubt that they are the optical counterparts of 1H 0542−407 and H0534−581. This conclusion is consistent with the relative X-ray and optical luminosities of the two CVs. From their 2–10 keV *HEAO 1* fluxes and our optical photometry, we deduce $L_x/L_{opt} \approx 2$ for both objects (using the procedure of Bradt, Doxsey, and Jernigan 1978, and assuming no X-ray absorption or optical reddening; see below). This value is in good agreement with that expected for cataclysmic vari-

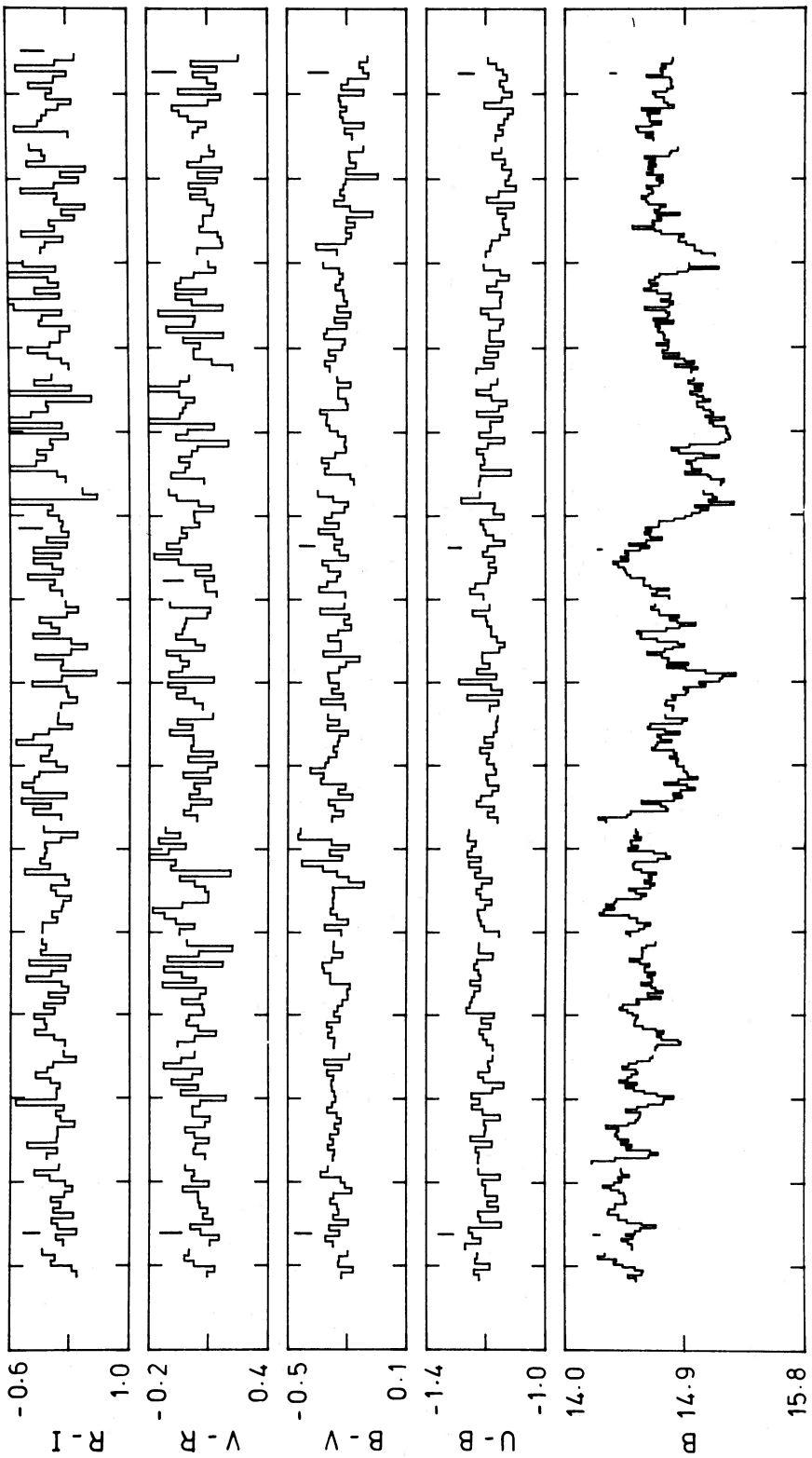

FIG. 15c

ables (Patterson 1981). Patterson and Raymond (1985*a*) show that such a value is expected empirically for cataclysmic variables with EW(Hβ) $\approx$ 45 Å (cf. Table 1).

We note that neither of the cataclysmic variables appears in catalogs of emission-line objects or variable stars (e.g., the *General Catalog of Variable Stars*; Kukarkin *et al.* 1969, and later supplements). The colors of the two new objects place them close to the blackbody curve for $T \gtrsim 25{,}000$ K. In fact, they lie at the extreme blue end of the two-color diagram for cataclysmic variables (Warner 1976; Bruch 1984), indicating low reddening (which is consistent with the low or moderate $N_{\rm H}$ inferred from their *EXOSAT* spectra). The absence of appreciable reddening suggests that far-UV emission should be detectable with *IUE*. In particular, it will be interesting to test the prediction for optically thin recombination that the intensity of He II λ1640 is about 7 times that of He II λ4686 (Patterson and Raymond 1985*b*).

Patterson (1984) has demonstrated a reasonable correlation between EW(Hβ) and the absolute visual magnitude of the accretion disk for systems with EW(Hβ) > 15 Å. From this relation we can estimate that $M_v = 9.4 \pm 1$ for 1H 0542−407, and $M_v = 9.1 \pm 1$ for H0534−581. Using their mean observed magnitudes, we can predict distances to within a factor of 2 of 180 and 140 pc, corresponding to X-ray luminosities of 8 and 7×10^{31} ergs s^{-1} (2–10 keV), respectively. These luminosities are similar to other nova-like X-ray emitters such as 2A 0526−328 (TV Col), 3A 0729+103 (BG CMi), and 2A 1150+72 (YY Dra), which were all first discovered via their hard X-ray emission (cf. Patterson 1984, and references therein).

Discussion specific to each cataclysmic variable follows.

a) 1H 0542−407

Our detection of soft X-ray and optical pulsations from 1H 0542−407 immediately establishes this object as a new member of the DQ Herculis class of magnetic variables (see reviews by Warner 1983, 1985; and Mason 1985). These systems differ from the AM Herculis magnetic variables in that their white dwarf rotation periods are not synchronized with their orbital periods. A further fundamental difference is that an accretion disk, as well as an accretion funnel, may be present in DQ Her systems. As a consequence of the asynchronous rotation, X-ray pulsations associated with an emission region at the base of the accretion funnel are seen as the white dwarf rotates (in addition to possible orbital modulation of the X-ray flux). The white dwarf rotation period may also be evident at optical wavelengths, although a sideband period resulting from reprocessing of the X-ray pulsations in a region corotating with the orbital velocity is often more prominent. Possible reprocessing sites include the atmosphere of the companion star and a bulge in the outer region of an accretion disk. It is thought that the magnetic fields in DQ Her systems are a factor $\sim$10 lower than in AM Her systems (Lamb and Patterson 1983; Lamb 1985). The absence of significant circular polarization from 1H 0542−407 is consistent with this conclusion.

We interpret the pronounced 1920 s soft X-ray periodicity in 1H 0542−407 as the rotation period of the white dwarf. The large pulse fraction at 0.1–1 keV, decreasing toward higher energies, is similar to the behavior seen in other DQ Her systems (Mason 1985). As noted earlier (§ III*b*), the 1920 s soft X-ray (0.1–1 keV) light curve is sinusoidal in shape, while the hard X-ray (1–9 keV) profile has a flatter X-ray maximum and a narrow minimum. King and Shaviv (1984; see also Hameury, King, and Lasota 1986) interpret the sinusoidal X-ray modulation in DQ Herculis systems as being due to an emission polecap which occupies a large fraction ($f > 0.25$) of the white dwarf's surface. In contrast, Lamb (1985) argues that the emitting fraction is much smaller ($f \ll 1$), and that the X-ray pulse profile is influenced by the large difference between the lateral and radial opacity of the accretion funnel. For example, Imamura (1984) has produced soft and hard X-ray light curves similar to those of Figure 7 by modeling the polar accretion on to AM Herculis, for which $f \ll 1$ (see also Imamura and Durisen 1983). A further possibility (pointed out by the referee) which could lead to sinusoidal modulation for $f \ll 1$ is that the X-ray emission is distributed as an arc in longitude on the surface of the white dwarf. Such an emission pattern having a small extent in latitude might arise if the accretion of material on to the magnetic white dwarf occurs via an accretion disk.

The second X-ray period of $\sim$6.2 hr in 1H 0542−407 must represent the orbital period of the system. Such a period is reasonably close to that expected from the empirical distribution of rotation periods versus orbital periods for the other known DQ Herculis stars (Lamb and Patterson 1983). The mechanism responsible for the approximately sinusoidal orbital modulation is unclear. Occultation of the white dwarf by the secondary star can be ruled out however, since this would produce a narrow eclipse similar to that reported in EX Hya (Córdova, Mason, and Kahn 1985). The X-ray modulation may be caused by obscuration of the white dwarf by a region in the accretion disk (if present). In this event, we would expect the modulation amplitude in the LE1 data to dominate that for the ME because of soft X-ray absorption. This does not seem to be the case, at least in the first $\sim$6.2 hr cycle in the ME data (§ III*b*). The available data therefore suggest that the mechanism responsible for the amplitude modulation of the X-ray pulsations is not a strong function of energy.

The optical periodicity of 1980 ± 35 s that we measure from 1H 0542−407 lies between the rotation period of 1920 s and the sideband optical period of $\sim$2100 s that might arise as a result of beating between the rotation and orbital periods. This suggests that the 1980 s periodicity may in reality correspond to an unresolved blend of the aforementioned periods. If so, the 1920 s optical component would seem to be dominant and must be produced near the white dwarf, while two explanations appear possible for the $\sim$2100 s component. First, reprocessing of the X-ray pulsations in material corotating with the orbital velocity is known to produce an optical beat period in other DQ Herculis systems. Second, the $\sim$2100 s component might simply be a consequence of orbital amplitude modulation of the optical pulsations from the white dwarf (i.e., by the same mechanism producing the amplitude modulation of the X-ray pulsations). In both cases we would expect the $\sim$1920 s and $\sim$2100 optical periodicities to be resolved by photometric measurements over a suitably long time base.

In comparison with other DQ Her systems, 1H 0542−407 most closely resembles TV Col (2A 0526−328) which has a white dwarf rotation period of 1943 s and an orbital period of 5.49 hr (Schrijver *et al.* 1985). TV Col also exhibits two other periods at optical wavelengths; an unexplained photometric period of 5.25 hr and an associated beat period (with the 5.49 hr spectroscopic period) of $4^{\rm d}.02$. It will be interesting to determine whether 1H 0542−407 displays an equally complex range of optical periodicities. In common with 1H 0542−407, TV Col undergoes X-ray modulation at the orbital period, but

it is clear from correlated spectral changes that the modulation in TV Col is caused by variable absorption. The average absorption for TV Col is very high ($N_H \approx 4 \times 10^{22}$ cm^{-2}) and no soft X-ray (< 1 keV) pulsations are detectable, in contrast to the large pulse fraction of ~70% for 1H 0542−407. Soft X-ray pulsations have in fact only been observed in one other DQ Her system, namely EX Hya which has a lower pulse fraction of ~30% (Córdova, Mason, and Kahn 1985).

Apart from the low absorption, the X-ray spectrum of 1H 0542−407 is comparable to the hard X-ray spectra observed from other DQ Her systems. For instance, H2252−035 can be characterized by a thermal spectrum with $kT > 20$ keV, and an iron line of equivalent width ~0.56 keV (White and Marshall 1981). It seems likely that the strong iron line emission detected from H2252−035, EX Hya (Watson 1985), and now 1H 0542−407 can be attributed to fluorescent excitation in the accretion funnel by high-energy X-rays, in a manner analogous to AM Her (Swank, Fabian, and Ross 1984).

b) *H0534−581*

The absence of distinctive X-ray or optical properties makes a classification of H0534−581 difficult. Nevertheless, the moderately strong He II λ4686 emission suggests that the object is a nova-like variable or a magnetic CV of the AM Her or DQ Her type (cf. Watts 1985). We do not favor an AM Her classification, however, for the following reasons. First, the object does not undergo pronounced and repeatable orbital modulation with a period of 1–4 hr, which is a characteristic of the 11 known AM Her systems. Second, the lack of a flickering color correlation contrasts with the dramatic color-dependent flickering behavior of AM Her (Priedhorsky and Krzeminski 1978). Third, our LE1 observations by *EXOSAT* show that H0534−581 does not have the soft X-ray excess expected for an AM Her variable.

H0534−581 might be a DQ Her system, despite our failure to detect strong X-ray pulsations with *EXOSAT*. The pulsations could be reduced in amplitude by such factors as insufficient misalignment between the emitting magnetic pole and the rotation axis of the white dwarf, or by destructive interference of the antiphased emission from both magnetic poles (e.g., King and Shaviv 1984). In the latter case, it is conceivable that optical pulsations might still be detectable, depending on the location of a suitable X-ray reprocessing site in the binary system (for instance, pulsations such as those observed in our photometry of 1984 November 17 and 18; § IV*c*). We remark that the hard X-ray spectrum of H0534−581 is consistent with a DQ Her classification.

V. SUMMARY REMARKS

We have established that the *HEAO 1* sources 1H 0542−407 and H0534−581 are cataclysmic variables. Both objects have very hard X-ray spectra and are variable by >1.5 mag at optical wavelengths. 1H 0542−407 is a new member of the DQ Herculis class of magnetic variables and has a white dwarf rotation period of ~1920 s and an orbital period near 6.2 hr. Optical pulsations at a centroid period of ~1980 s indicate emission from near the white dwarf and possibly from an X-ray reprocessing site elsewhere in the binary system. The CV subclass of H0534−581 is uncertain, although an AM Herculis classification is ruled out. It is most likely a nova-like variable or perhaps a DQ Herculis system in which the X-ray pulsations are below our detection threshold.

Last, we remark that a program of high-speed photometry and radial velocity measurements is in progress for both cataclysmic variables. It is expected that these observations will allow detailed modeling of 1H 0542−407 and hopefully resolve the nature of H0534−581.

We are especially grateful to the European Space Agency for allocating *EXOSAT* time to observe the two cataclysmic variables. I. R. T. wishes to thank the *EXOSAT* team at ESOC, Darmstadt for their generous advice and hospitality during his visit, especially M. Gottwald, A. Parmar, L. Stella, and N. White. The assistance of Anne Fahey in scheduling the coordinated X-ray and optical observations is greatly appreciated.

The excellent support provided by the technical staffs of the ANU, AAO, and CTIO is acknowledged. I. R. T. and D. A. H. B. particularly thank Professor Don Mathewson for granting observing time during the commissioning phase of the ANU 2.3 m telescope and also Drs. Visvanathan and Wickramasinghe for sharing observing time to obtain the spectropolarimetry of 1H 0542−407. I. R. T. and H. B. are grateful to participants at the Time Variability Workshop in Taos, N.M. for enlightening discussions, particularly F. Córdova, D. Lamb, K. Mason, and M. Watson. We thank the Australian Department of Science and the US National Science Foundation for their support under the US/Australia Bilateral Science and Technology Agreement. R. A. R., H. V. B., and D. A. S. acknowledge partial support by NASA contracts NAS8-27972 and NAS8-30453, by NASA grants NAG8-493 and NAG8-496, by NSF grants INT 82-11357, and AST 84-14591, and by the Smithsonian Institution Scholarly Studies Program.

REFERENCES

Bessell, M. S. 1986, *Pub. A.S.P.*, to be submitted.
Bradt, H. V., Doxsey, R. E., and Jernigan, J. G. 1978, in *X-ray Astronomy*, ed. W. A. Baitty and L. E. Peterson (Oxford: Pergamon), p. 3.
Bruch, A. 1984, *Astr. Ap. Suppl.*, **56**, 441.
Buckley, D. A. H., Tuohy, I. R., Remillard, R. A., Bradt, H. V., and Schwartz, D. A. 1986, *Ap. J.*, submitted.
Córdova, F. A., Mason, K. O., and Kahn, S. M. 1985, *M.N.R.A.S.*, **212**, 447.
de Korte, P. A. J., *et al.* 1981, *Space Sci. Rev.*, **30**, 495.
Graham, J. A. 1982, *Pub. A.S.P.*, **94**, 244.
Gursky, H., *et al.* 1978, *Ap. J.*, **223**, 973.
Hameury, J. M., King, A. R., and Lasota, J. P. 1986, *M.N.R.A.S.*, **218**, 695.
Imamura, J. N. 1984, *Ap. J.*, **285**, 223.
Imamura, J. N., and Durisen, R. H. 1983, *Ap. J.*, **268**, 291.
King, A. R., and Shaviv, G. 1984, *M.N.R.A.S.*, **211**, 883.
Kukarkin, B. V., *et al.* 1969, *General Catalog of Variable Stars* (3d ed.; Moscow).
Lamb, D. Q. 1985, in *Cataclysmic Variables and Low Mass X-Ray Binaries*, ed. D. Q. Lamb and J. Patterson (Dordrecht: Reidel), p. 179.
Lamb, D. Q., and Patterson, J. 1983, in *IAU Colloquium 72, Cataclysmic Variables and Related Objects*, ed. M. Livio and G. Shaviv (Dordrecht: Reidel), p. 229.
Landolt, A. V. 1983, *A.J.*, **88**, 439.
McClean, I. S., Heathcote, S. R., Paterson, M. J., Fordham, J., and Shortridge, K. 1984, *M.N.R.A.S.*, **209**, 655.
Marshall, F. E., Boldt, E. A., Holt, S. S., Mushotzky, R. F., Pravdo, S. H., Rothschild, R. E., and Serlemitsos, P. J. 1979, *Ap. J. Suppl.*, **40**, 657.
Mason, K. O. 1985, *Space Sci. Rev.*, **40**, 99.
Oke, J. B. 1974, *Ap. J. Suppl.*, **27**, 21.
Patterson, J. 1981, *Nature*, **292**, 810.
———. 1984, *Ap. J. Suppl.*, **54**, 443.
Patterson, J., and Raymond, J. C. 1985*a*, *Ap. J.*, **292**, 535.
———. 1985*b*, *Ap. J.*, **292**, 550.

Priedhorsky, W. C., and Krzeminski, W. 1978, *Ap. J.*, **219**, 597.
Remillard, R. A., Bradt, H. V., Buckley, D., Roberts, W., Schwartz, D. A., Tuohy, I. R., and Wood, K. 1986, *Ap. J.*, **301**, 742.
Schrijver, J., Brinkman, A. C., van der Woerd, H., Watson, M. G., King, A. R., van Paradijs, J., and van der Klis, M. 1985, *Space Sci. Rev.*, **40**, 121.
Schwartz, D., Bradt, H., Buckley, D., Patterson, J., Remillard, R., Roberts, W., and Tuohy, I. 1984*a*, in *X-ray Astronomy '84*, ed. M. Oda and R. Giacconi (Tokyo: ISAS), p. 455.
———. 1985, *Adv. Space Res.*, **5**, 137.
Schwartz, D. A., Schwarz, J., Gursky, H., Bradt, H., and Doxsey, R. E. 1978, in *Proc. AIAA 16th Aerospace Science Conf.*, p. 78.
Schwartz, D. A., *et al.* 1984*b*, *Bull. AAS*, **16**, 514.
Stella, L., Kahn, S. M., and Grindlay, J. E. 1984, *Ap. J.*, **282**, 713.
Swank, J. H., Fabian, A. C., and Ross, R. R. 1984, *Ap. J.*, **280**, 734.
Tuohy, I. R., Buckley, D. A. H., Remillard, R. A., Bradt, H. V., and Schwartz, D. A. 1985, in *Recent Results on Cataclysmic Variables* (ESA SP-236), p. 73.
Turner, M. J. L., Smith, A., and Zimmerman, H. U. 1981, *Space Sci. Rev.*, **30**, 513.
Warner, B. 1976, in *IAU Symposium 73, The Structure and Evolution of Close Binary Systems*, ed. P. Eggleton, S. Mitten, and J. Whelan (Dordrecht: Reidel), p. 85.
———. 1983, in *Cataclysmic Variables and Related Objects*, ed. M. Livio and G. Shaviv (Dordrecht: Reidel), p. 155.
———. 1985, in *Cataclysmic Variables and Low Mass X-Ray Binaries*, ed. D. Q. Lamb and J. Patterson (Dordrecht: Reidel), p. 269.
Watson, M. G. 1985, talk presented at the Los Alamos Workshop on "Time Variability in X-ray and γ-ray Sources."
Watts, D. 1985, in *Recent Results on Cataclysmic Variables* (ESA SP-236), p. 259.
White, N. E., and Marshall, F. E. 1981, *Ap. J.* (*Letters*), **249**, L25.
Wood, K. S., *et al.* 1984, *Ap. J. Suppl.*, **56**, 507.

H. V. BRADT and R. A. REMILLARD: Center for Space Research, Massachusetts Institute of Technology, Cambridge, MA 02139

D. A. H. BUCKLEY and I. R. TUOHY: Mount Stromlo and Siding Spring Observatories, Woden P.O., ACT 2606, Australia

D. A. SCHWARTZ: Harvard-Smithsonian Center for Astrophysics, 60 Garden Street, Cambridge, MA 02138